Theoretical and experimental study of crack modes of flow elastoplasticity

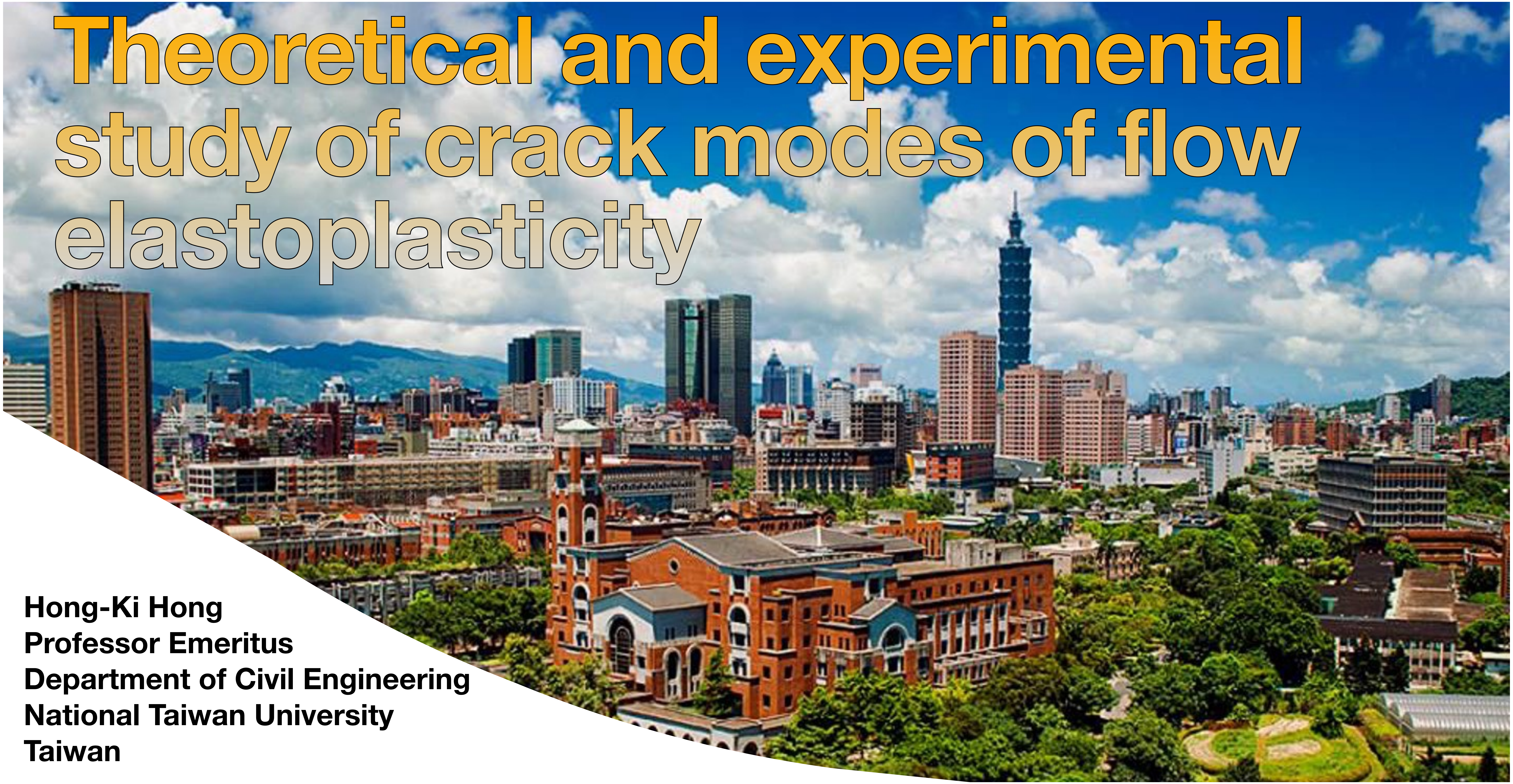

Hong-Ki Hong
Professor Emeritus
Department of Civil Engineering
National Taiwan University
Taiwan

Overview

- Experimental evidence of yield surface evolution
- A model with evolving cubic distortional yield hypersurface
- Yield surface evolution under strain-controlled paths
- Yield surface evolution under stress-controlled paths
- Study of crack of flow elastoplasticity
- Conclusions

Experimental evidence of yield surface evolution

Yield surfaces in 2D space

Pure aluminum (Phillips & Tang 1972)

Initial yield surface

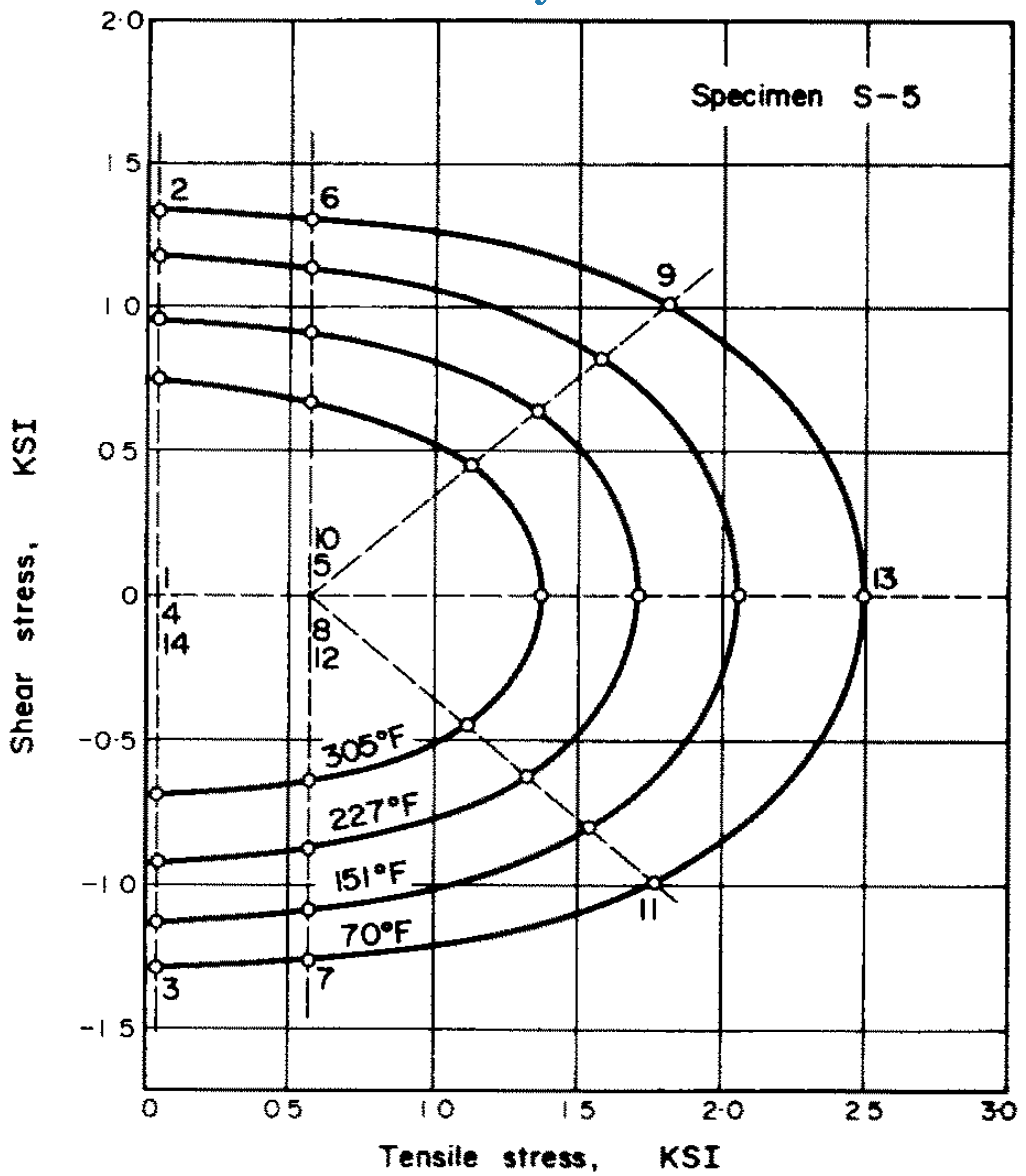

Subsequent yield surfaces under axial prestress

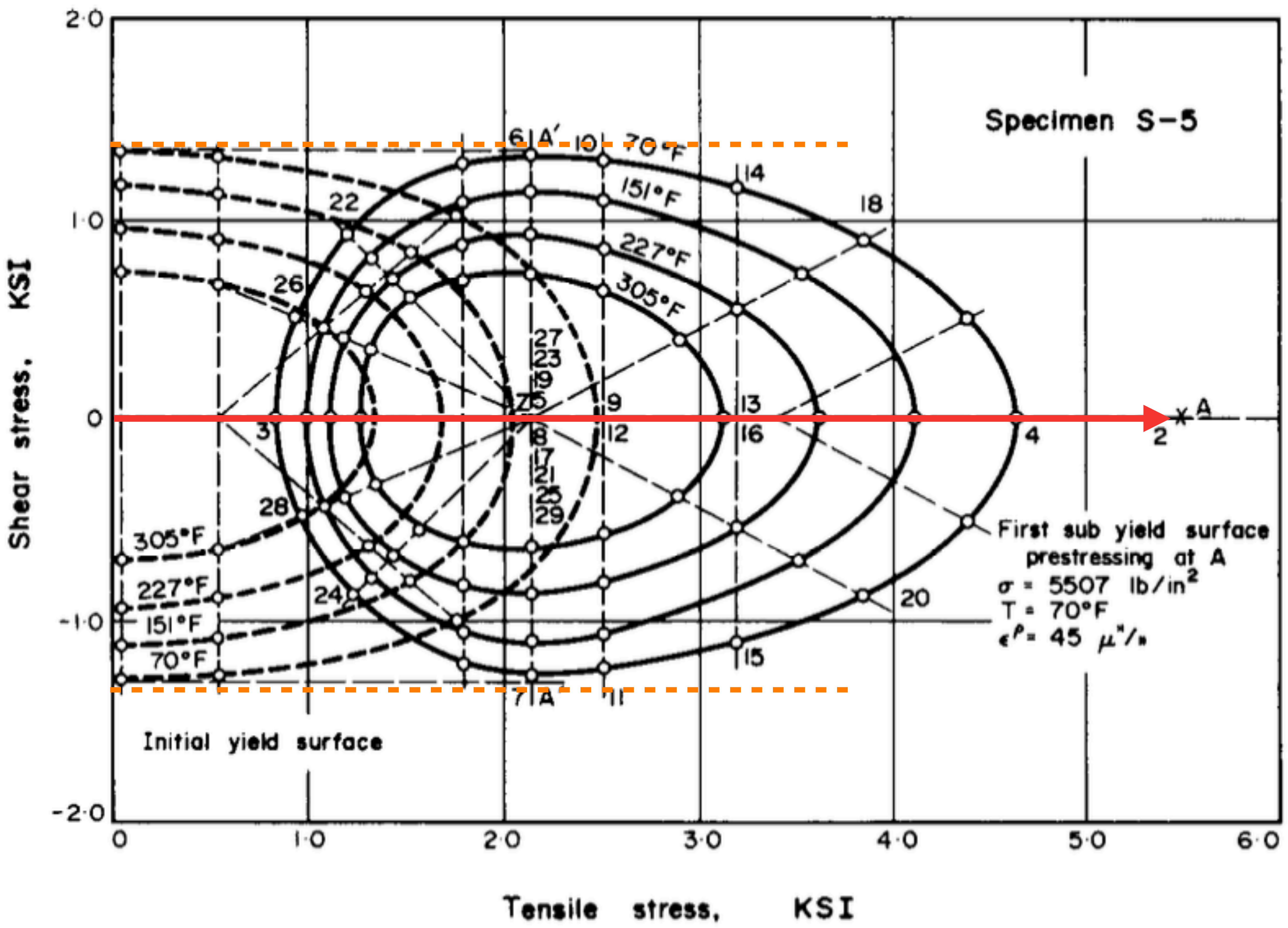

• A. Phillips, J.-L. Tang, The effect of loading path on the yield surface at elevated temperatures, International Journal of Solids and Structures, Vol. 8, pp. 463-474, 1972.

Yield surfaces in 2D space

Pure aluminum (Phillips & Tang 1972)

Subsequent yield surfaces

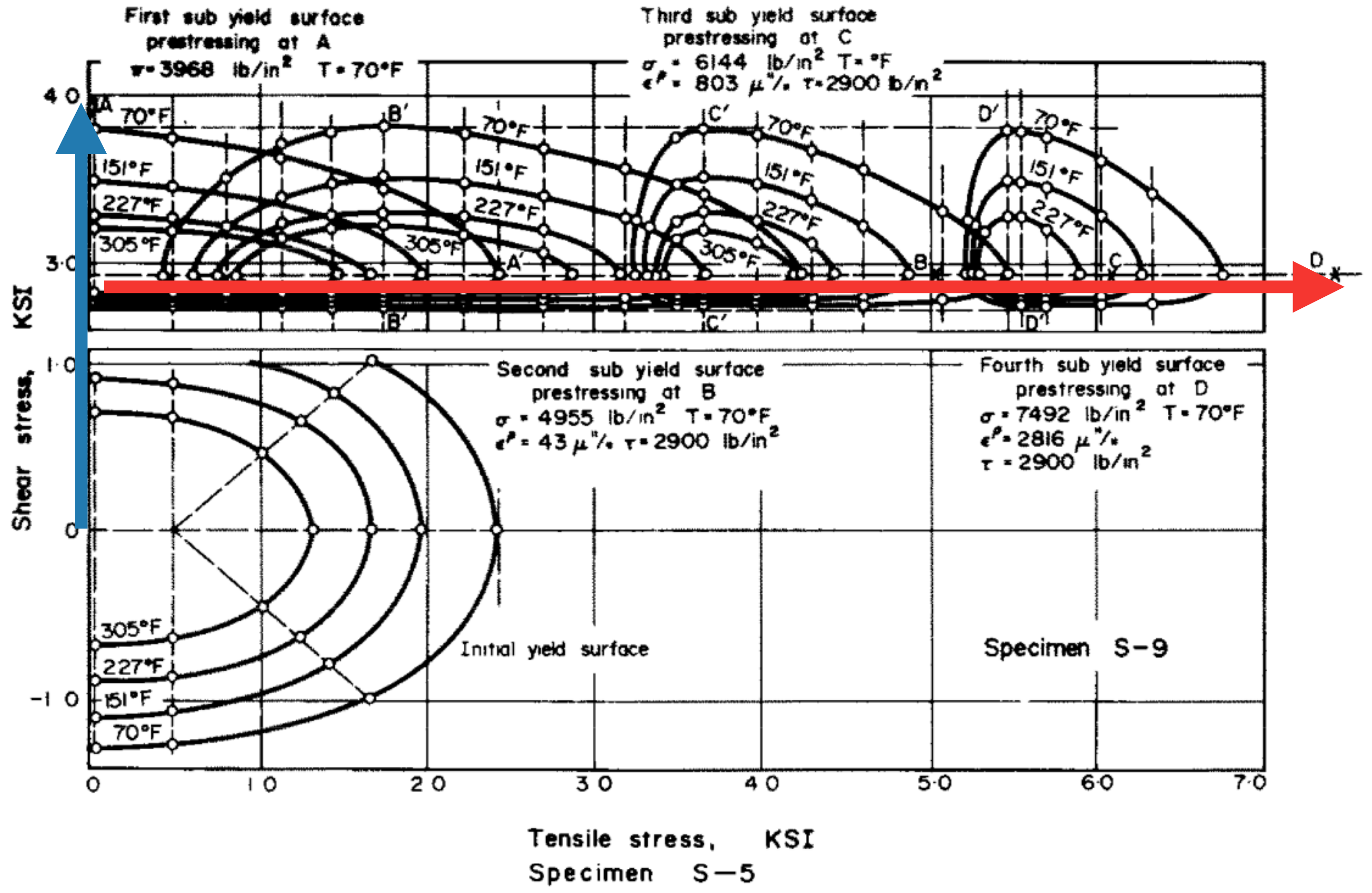

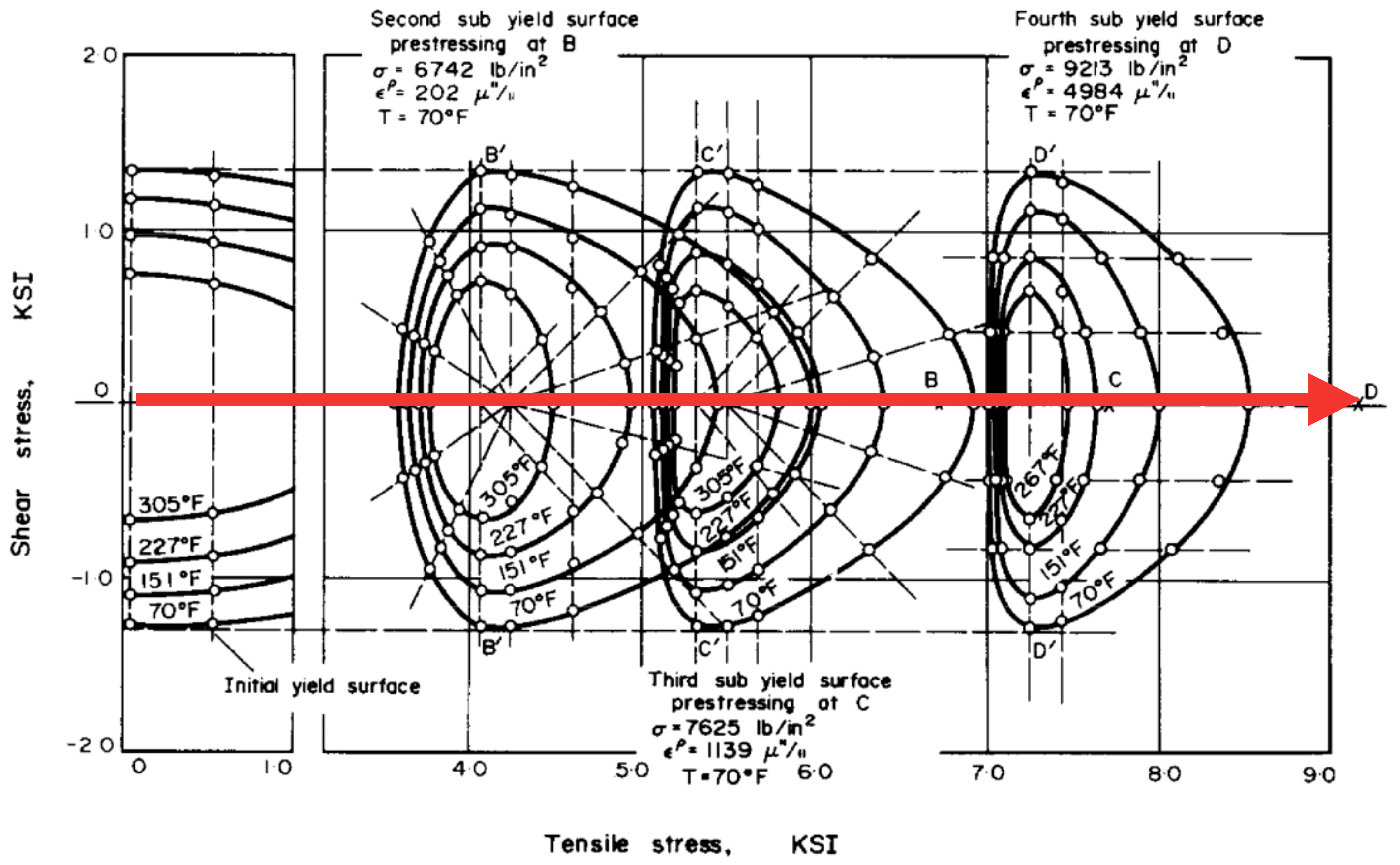

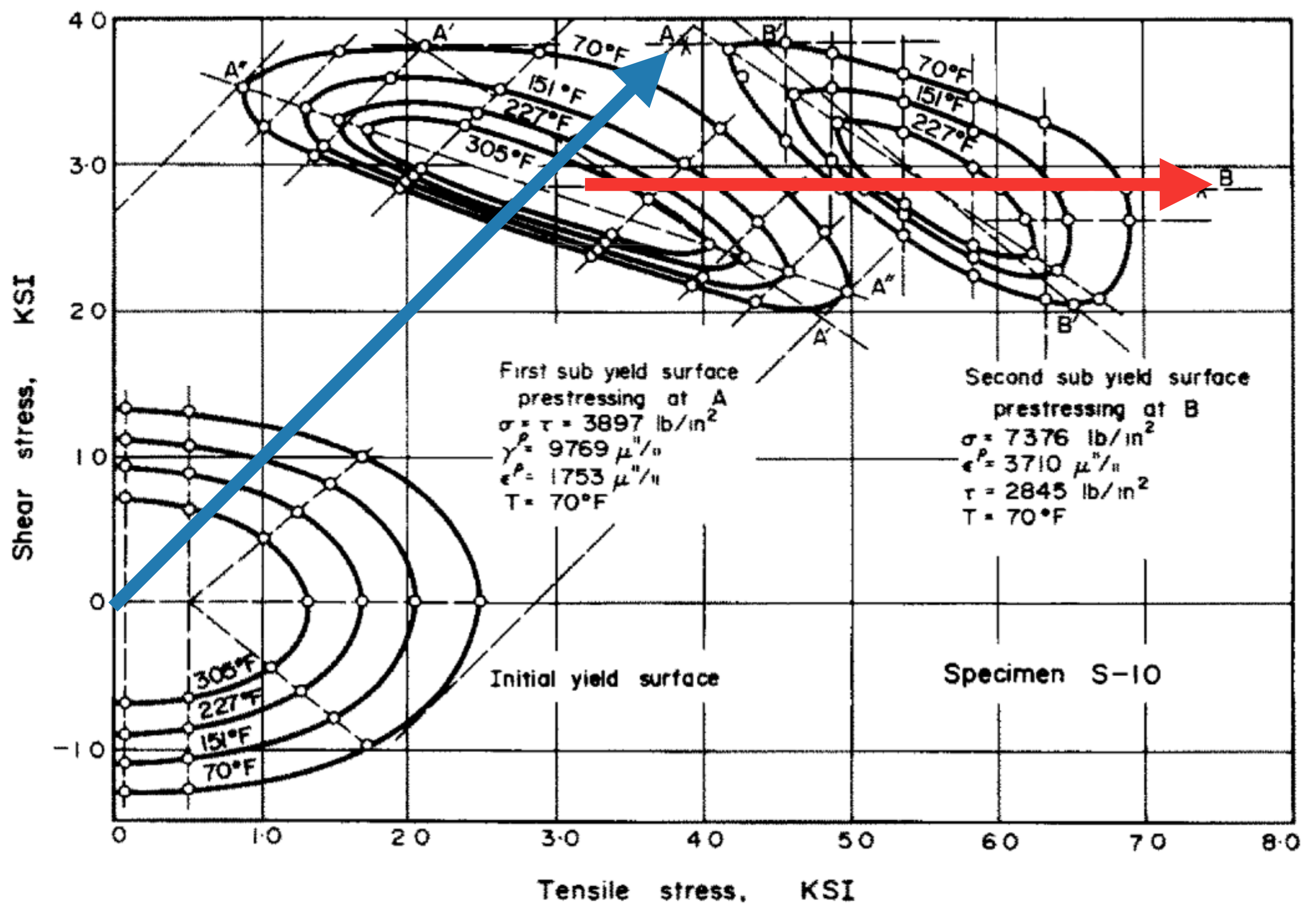

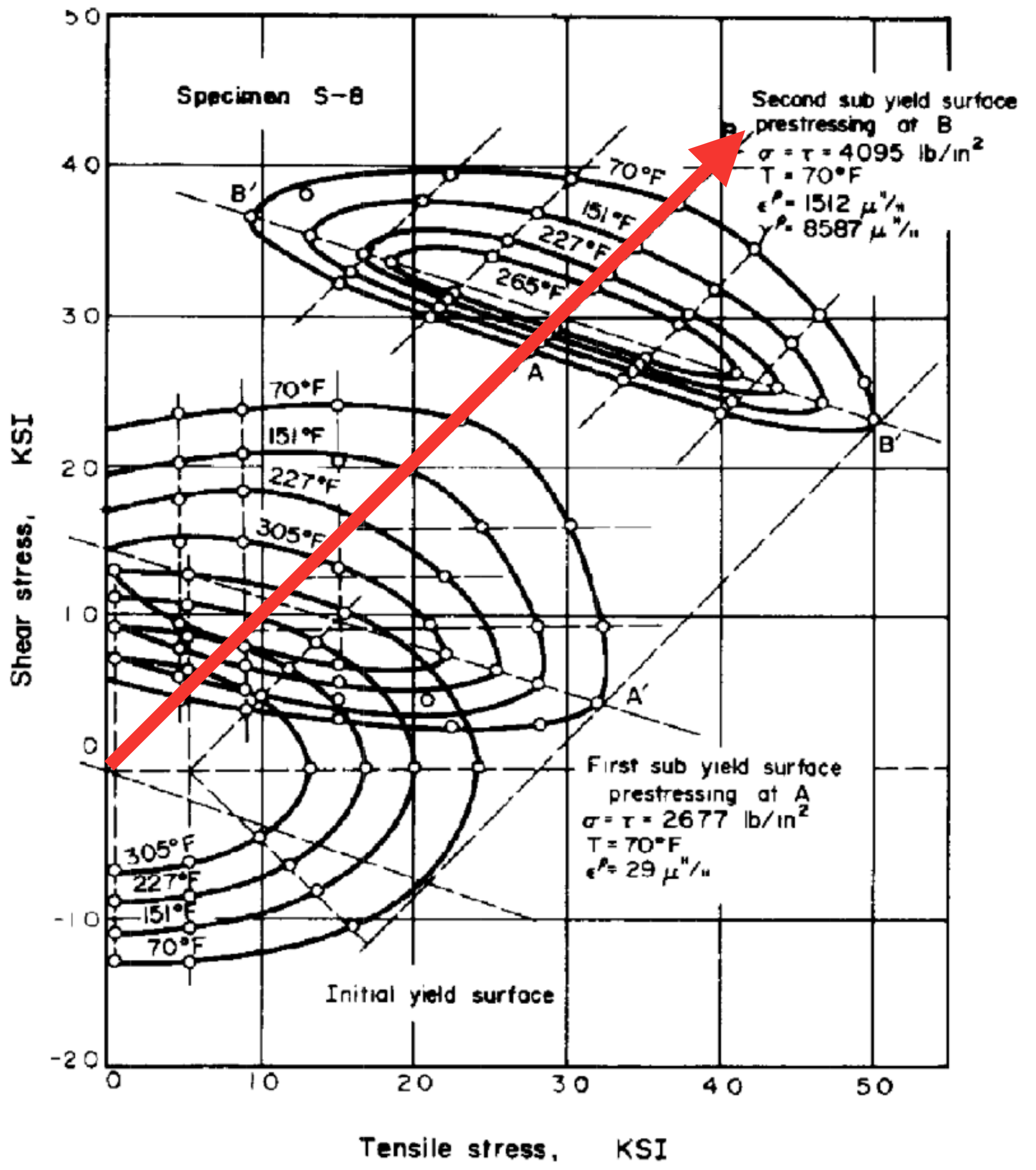

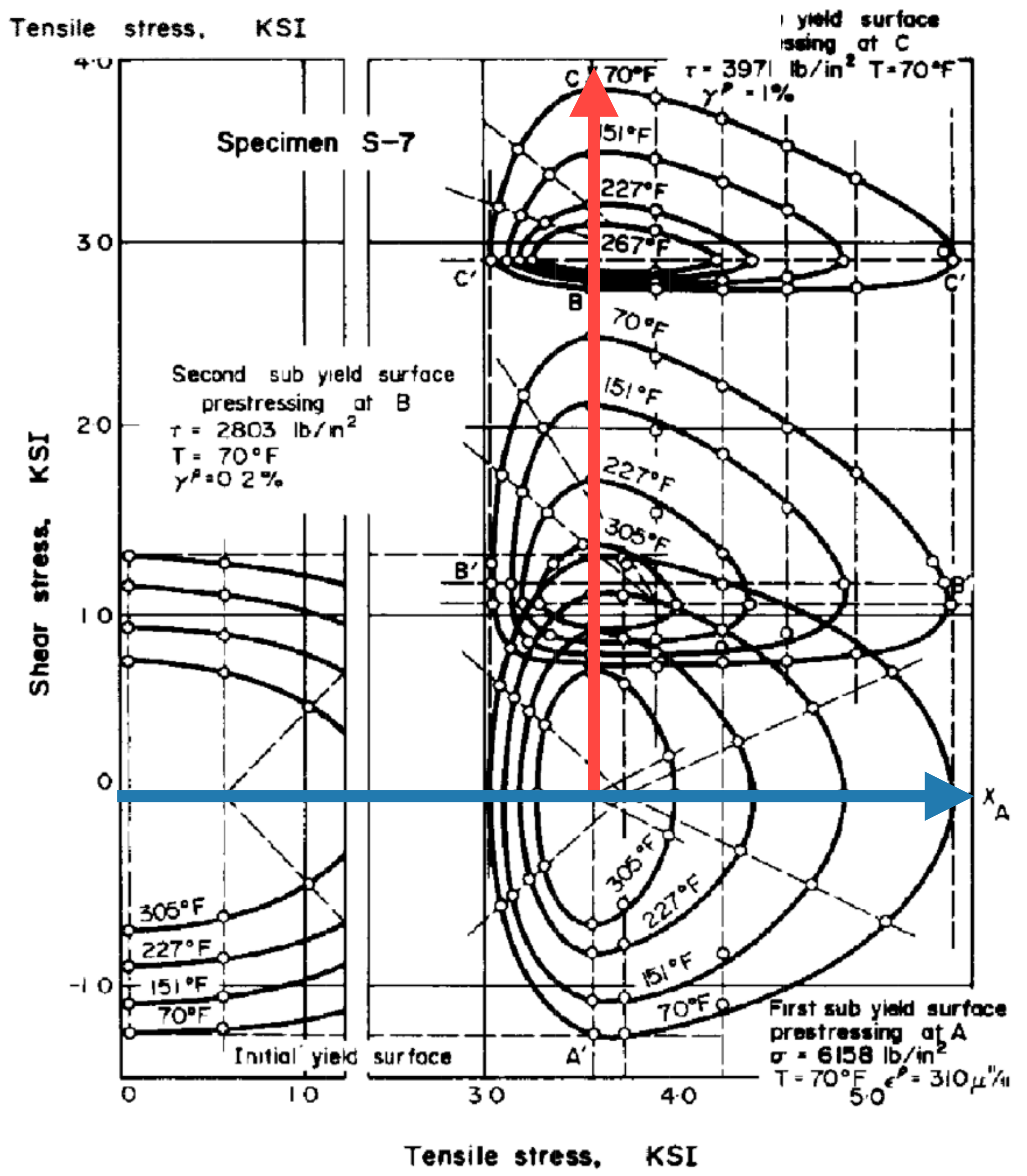

- A. Phillips, J.-L. Tang, The effect of loading path on the yield surface at elevated temperatures, International Journal of Solids and Structures, Vol. 8, pp. 463-474, 1972.

Yield surfaces in 2D space

Brass (Shiratori et al.1974)

Influence of preloading paths

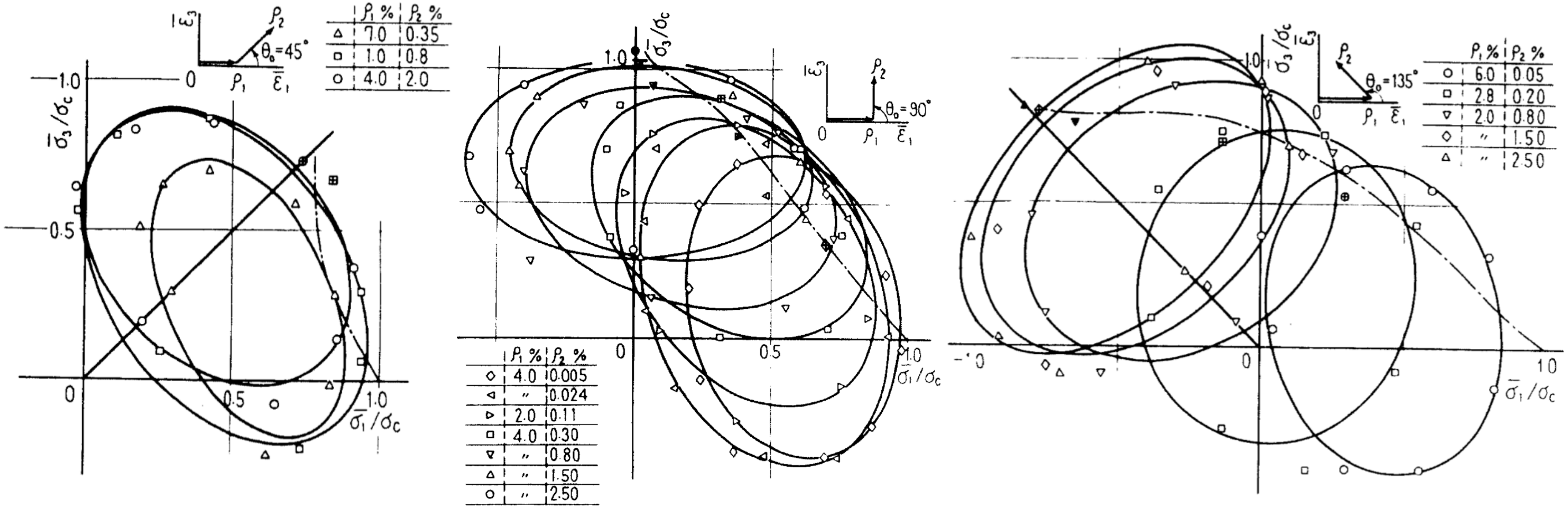

- E. Shiratori, K. Ikegami, K. Kaneko, The stress vector and the subsequent yield surface in loading along the strain path with a corner, Bulletin of JSME, Vol. 17, No. 113, 1405-1412, 1974.

Yield surfaces in 2D space

Al6061-T6511 Al alloy under finite strain preloading

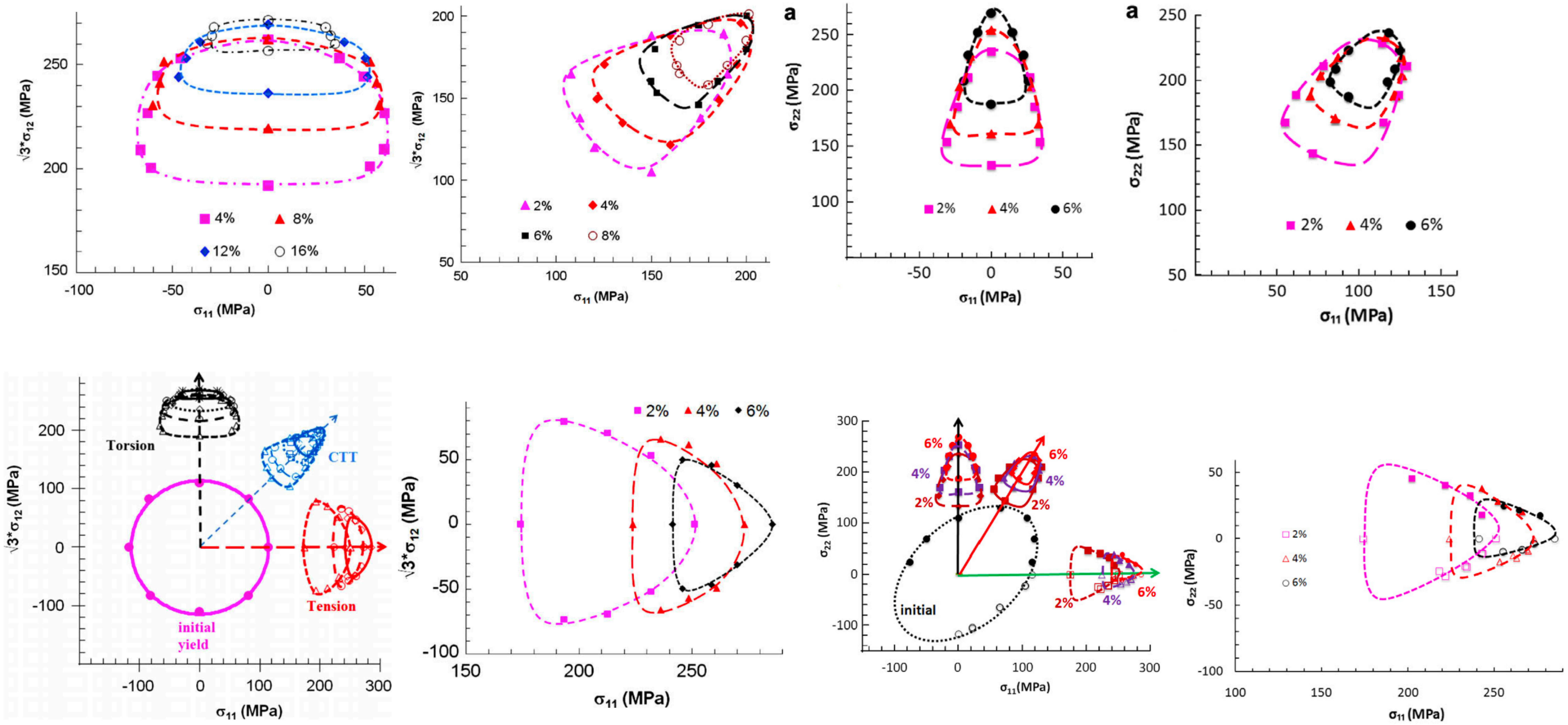

- A. S. Khan, R. Kazmi, A. Pandey, T. Stoughton, Evolution of subsequent yield surfaces and elastic constants with finite plastic deformation. Part-I: A very low work hardening aluminum alloy (Al6061-T6511), International Journal of Plasticity, Vol. 25, pp. 1611-1625, 2009.
- A. S. Khan, A. Pandey, T. Stoughton, Evolution of subsequent yield surfaces and elastic constants with finite plastic deformation. Part-III: Yield surface in tension–tension stress space (Al 6061–T 6511 and annealed 1100 Al) , International Journal of Plasticity, Vol. 26, pp. 1432-1441, 2010.

Yield surfaces in 2D space

SS304 Stainless steel (Wu & Yeh 1991)

Preloading path 1

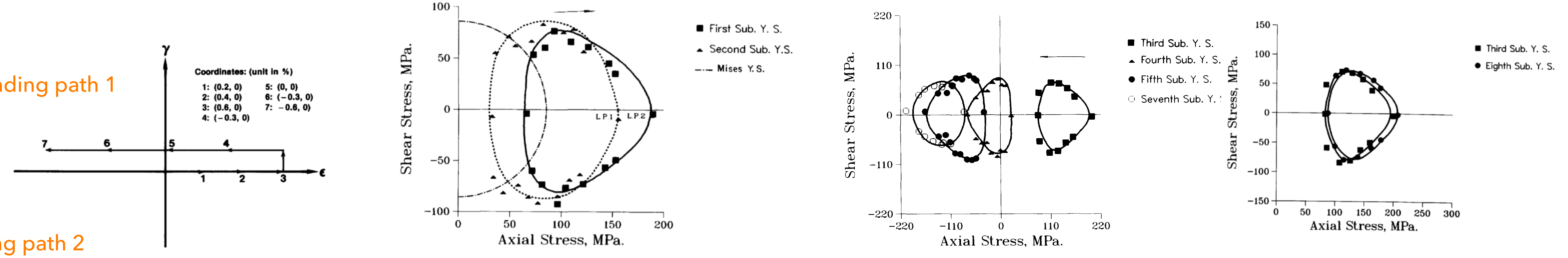

Preloading path 2

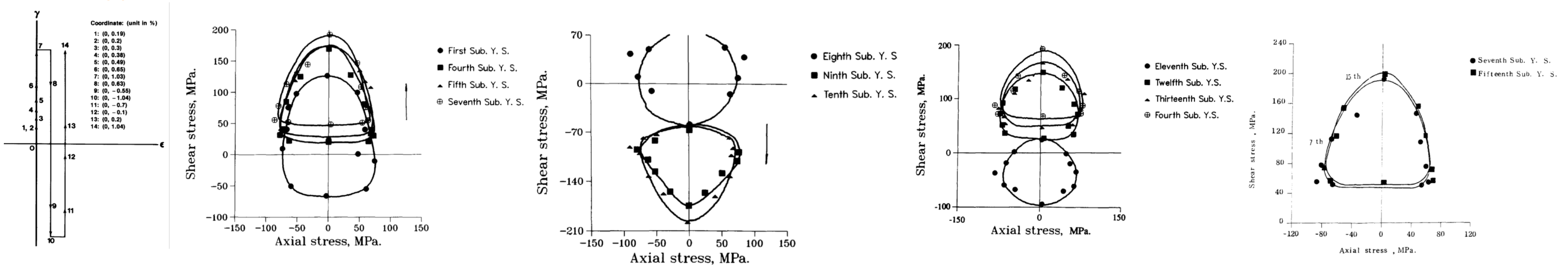

Preloading path 3

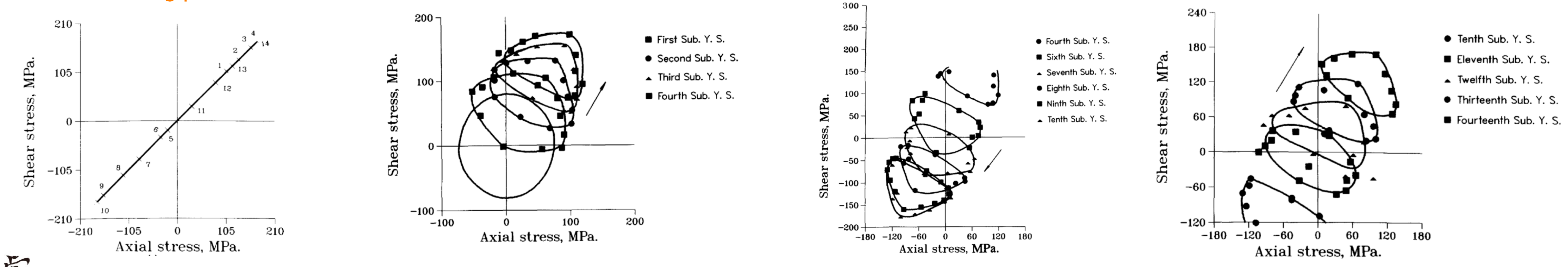

- H.-C. Wu, W. C. Yeh, On the experimental determination of yield surfaces and some results of annealed 304 stainless steel, International Journal of Plasticity, Vol. 7, pp. 803-826, 1991.

Yield surfaces in 3D space

Al1100 Al alloy (Phillips & Das 1985)

Initial yield surfaces

Plane $\sigma_{\theta\theta} = 0$

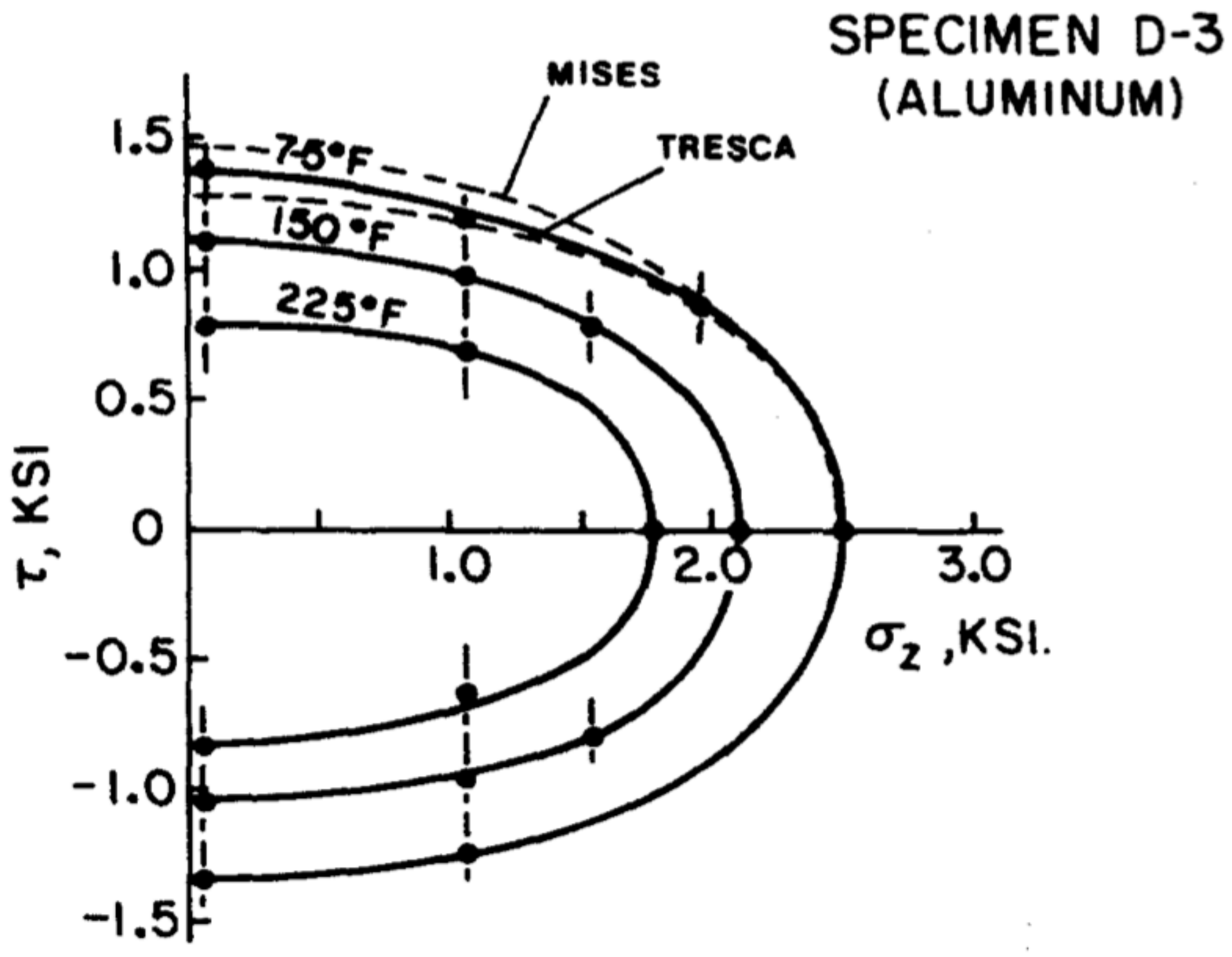

Plane $\sigma_{zz} = \sigma_{\theta\theta}/2 + 70$

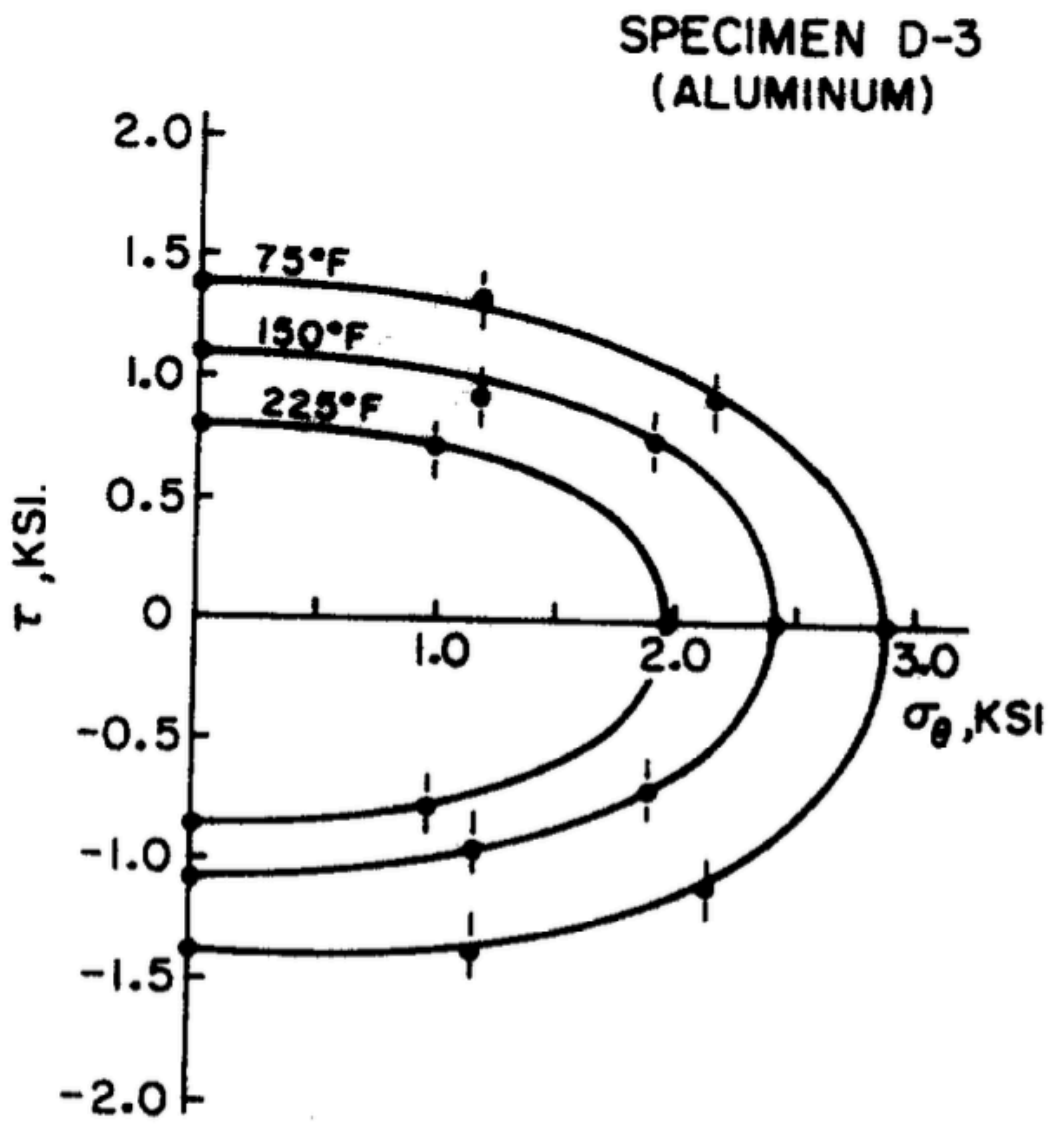

Plane $\sigma_{z\theta} = 0$

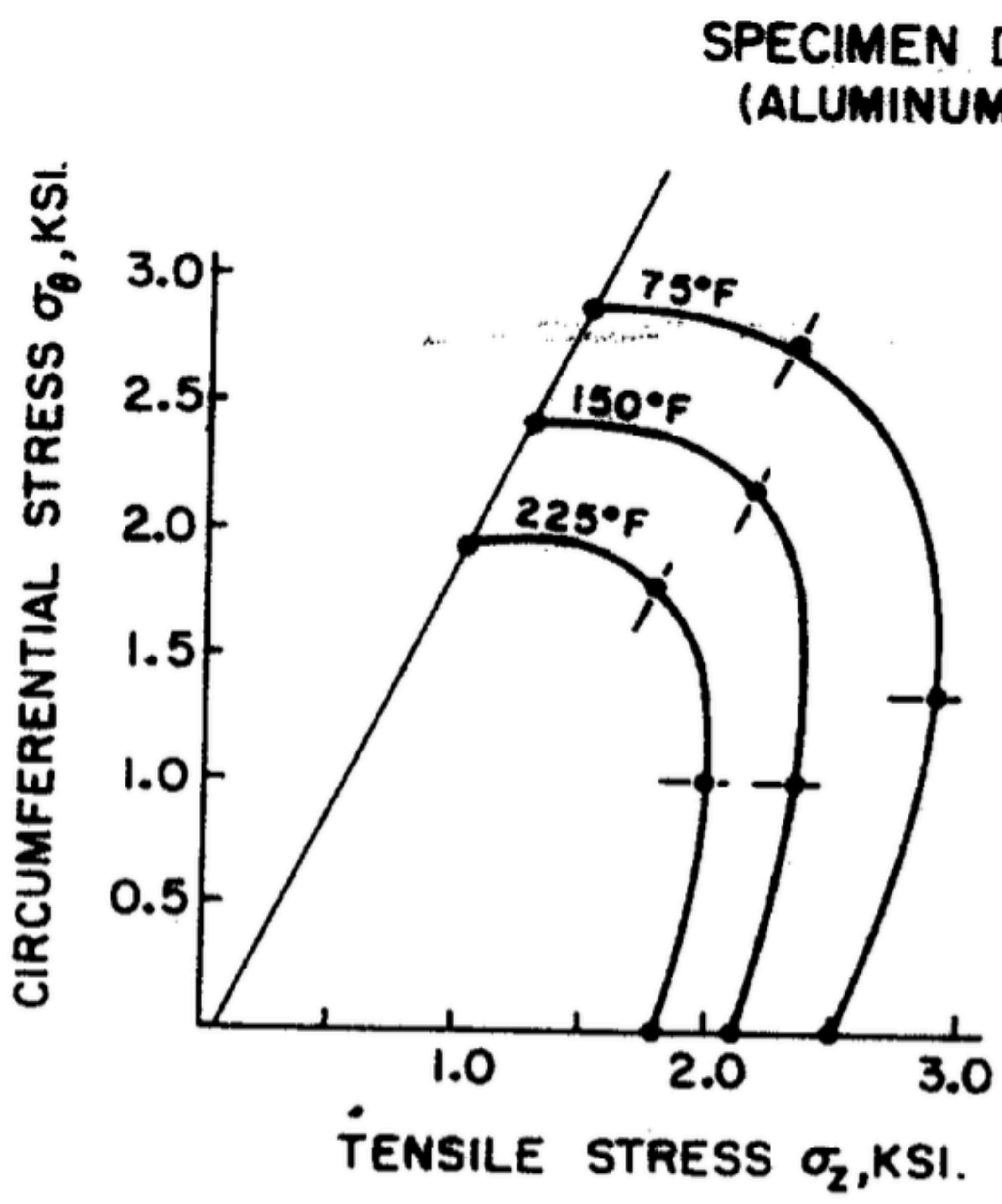

- A. Phillips, P. K. Das, Yield surfaces and loading surfaces of aluminum and brass: An experimental investigation at room and elevated temperatures, International Journal of Plasticity, Vol. 1, pp. 89-109, 1985.

A model with evolving cubic distortional yield hypersurface

Mathematical formulation

Elastic-plastic decompositions

$$\boldsymbol{\epsilon} = \boldsymbol{\epsilon}^{e\alpha} + \boldsymbol{\epsilon}^{p\alpha}, \quad \mathbf{e}, = \mathbf{e}^{e\alpha} + \mathbf{e}^{p\alpha}$$

Active-back decompositions

$$\boldsymbol{\sigma} = \boldsymbol{\sigma}_a + \boldsymbol{\sigma}_b, \quad \dot{\boldsymbol{\sigma}}^{\alpha} = \frac{R^{\alpha}(0)}{R^{\alpha}}\dot{\boldsymbol{\sigma}}_a^{\alpha} + \dot{\boldsymbol{\sigma}}_b^{\alpha} + \frac{k_p^{\alpha}\dot{\lambda}^{\alpha}}{\eta^{\alpha}}(\boldsymbol{\sigma}_b^{\alpha} - K tr \boldsymbol{\epsilon} \mathbf{1}), \quad \dot{\mathbf{s}}^{\alpha} = \frac{R^{\alpha}(0)}{R^{\alpha}}\dot{\mathbf{s}}_a^{\alpha} + \dot{\mathbf{s}}_b^{\alpha} + \frac{k_p^{\alpha}\dot{\lambda}^{\alpha}}{\eta^{\alpha}}\mathbf{s}_b^{\alpha},$$

Elastic constitutions

$$\dot{\mathbf{s}}_a^{\alpha} = 2G\dot{\mathbf{e}}^{e\alpha}, \text{tr}\, \boldsymbol{\epsilon} = \frac{1}{3K}\text{tr}\, \boldsymbol{\sigma}$$

Plastic flow rule

$$R_{\infty}^{\alpha}\dot{\mathbf{e}}^{p\alpha} = \mathbf{s}_a^{\alpha}\dot{\lambda}^{\alpha},$$

Kinematic hardening rules

$$\dot{\mathbf{e}}^{p\alpha} = \frac{1}{2G_p^{\alpha}}\dot{\mathbf{s}}_b^{\alpha} + \frac{1}{2\eta^{\alpha}}\mathbf{s}_b^{\alpha}\dot{\lambda}^{\alpha}$$

Stress admissible condition

$$R^{\alpha}(\lambda^{\alpha}) = R_{\infty}^{\alpha}\sqrt{1 - r^{\alpha}\ \exp\left(\frac{-2\lambda^{\alpha}}{\lambda_u^{\alpha}}\right)},$$

$$\Phi = \Phi(\boldsymbol{\sigma}_a) = \frac{\|\boldsymbol{\sigma}_a\|}{C} \leq 1$$

Non-negative dissipation

$$\dot{\lambda}^{\alpha} \geq 0,$$

$$\dot{\Lambda} = \left(\frac{1}{R_{\infty}^{s}}\|\mathbf{s}_a^{s}\|^2 + \frac{1}{2\eta^{s}}\|\mathbf{s}_b^{s}\|^2\right)\dot{\lambda}^{s} + \left(\frac{1}{R_{\infty}^{l}}\|\mathbf{s}_a^{l}\|^2 + \frac{1}{2\eta^{l}}\|\mathbf{s}_b^{l}\|^2\right)\dot{\lambda}^{l} \geq 0$$

Alternative conditions

$$\|\mathbf{s}_a^{\alpha}\|\dot{\lambda}^{\alpha} = R^{\alpha}(\lambda^{\alpha})\dot{\lambda}^{\alpha}, \quad \Phi\dot{\Lambda} = \dot{\Lambda}\,.$$

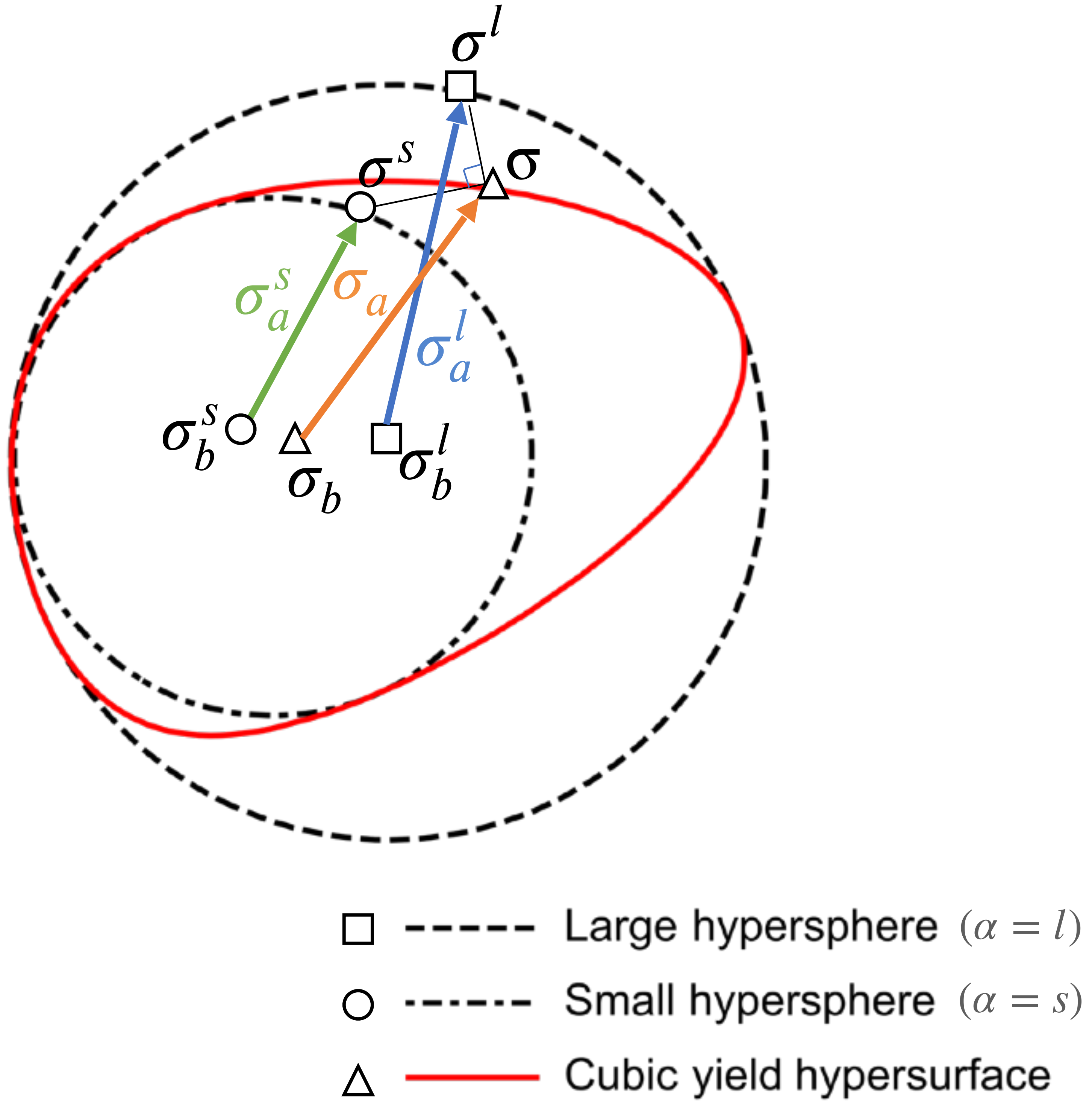

$0 < r^{\alpha} < 1$ hardening plasticity (the model behaves mixed-kinematic-isotropic hardening)

$r^{\alpha} = 0$ perfect plasticity (the model behaves purely kinematic hardening)

$r^{\alpha} < 0$ softening plasticity (the model behaves mixed-kinematic-isotropic softening)

10 material constants

$$E > 0, G > 0, r^{\alpha} < 1, R_{\infty}^{\alpha} > 0, G_p^{\alpha} > 0, \eta^{\alpha} > 0,$$

Hong-Ki Hong, Li-Wei Liu, Ya-Po Shiao, and Shao-Fu Yan, Axial-torsional strain-controlled experiments and an elastoplastic model with cubic distortional yield surface, Journal of Engineering Mechanics, 148(6), 04022027, 2022.

Internal symmetry

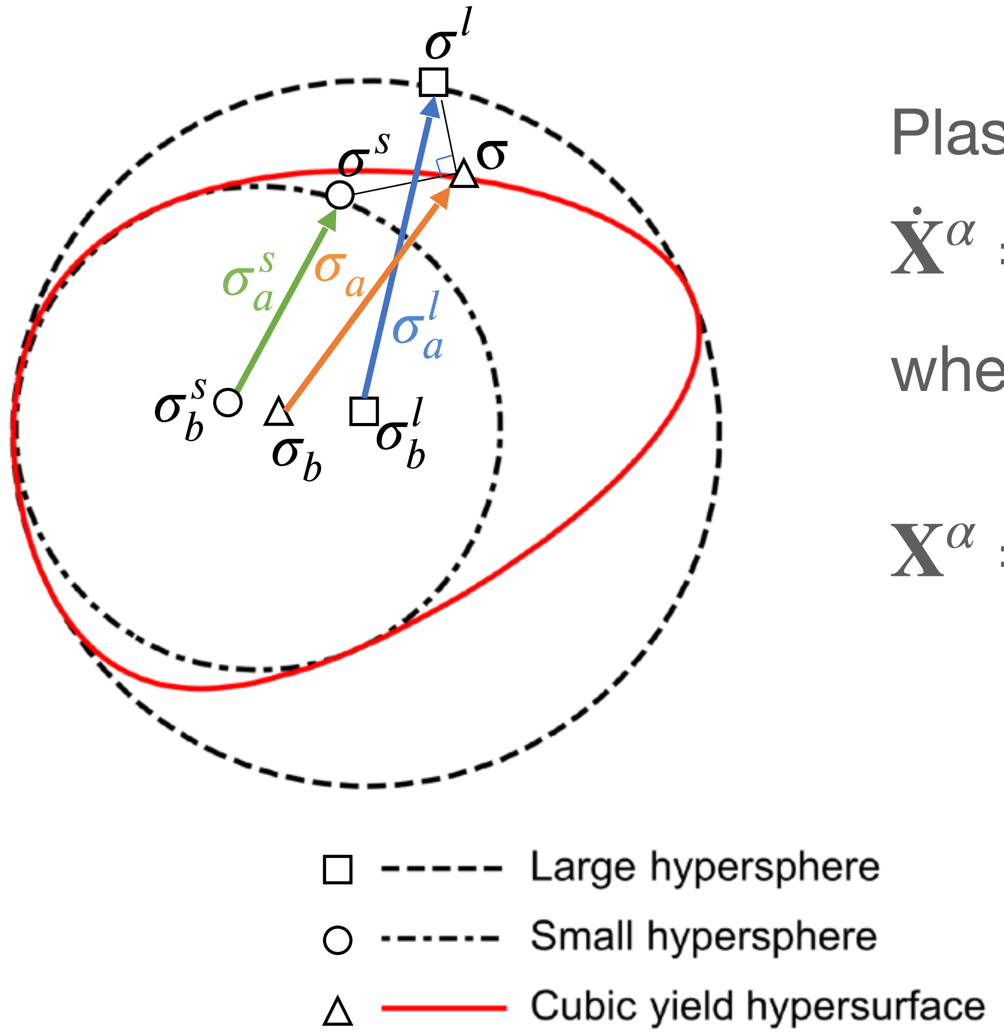

Plastic phase

$\dot{\mathbf{X}}^\alpha = \mathbf{A}_\alpha \mathbf{X}^\alpha$ Augmented stress $\mathbf{X}^\alpha$ space

where Deviatoric stress $\mathbf{s}_a^\alpha$ space

$$\mathbf{X}^\alpha = X_0^\alpha \begin{bmatrix} \frac{\mathbf{s}_a^\alpha}{R_\infty^\alpha} \\ 1 \end{bmatrix} \in \mathbb{R}^{6,1} \text{ and } \mathbf{A}_\alpha = \begin{bmatrix} \mathbf{0} & \dot{\mathbf{e}}/\lambda_u^\alpha \\ \dot{\mathbf{e}}^T/\lambda_u^\alpha & 0 \end{bmatrix} \in \mathrm{so}(6,1) \subset \mathbb{R}^{(6,1)\times(6,1)}$$

Internal symmetry

Two elements of the projective proper orthochronous Poincaré group $PSE_o(6,1)$ in the plastic phase and one element of the translation group T in the elastic phase

The solution $\mathbf{X}^\alpha(t) = \mathbf{G}_\alpha(t)\mathbf{G}_\alpha^{-1}(t_1)\mathbf{X}^\alpha(t_1) \quad \forall t, t_1 \in I_{on} \subset \mathbb{R}$

where $\mathbf{G}_\alpha \in SO_o(6,1)$,

$$\mathbf{G}_\alpha(t)\mathbf{G}_\alpha^{-1}(t_1) = \begin{bmatrix} \mathbf{I}_{6\times6} + ((a-1)/\|\dot{\mathbf{e}}\|^2)\dot{\mathbf{e}}\dot{\mathbf{e}}^T & b\dot{\mathbf{e}}/\|\dot{\mathbf{e}}\| \\ b\dot{\mathbf{e}}^T/\|\dot{\mathbf{e}}\| & a \end{bmatrix} \text{ and } a = \cosh[(t-t_1)\|\dot{\mathbf{e}}\|/\lambda_u^\alpha], \quad b = \sinh[(t-t_1)\|\dot{\mathbf{e}}\|/\lambda_u^\alpha].$$

國立臺灣大學 National Taiwan University

- Hong-Ki Hong, Li-Wei Liu, Ya-Po Shiao, and Shao-Fu Yan, Axial-torsional strain-controlled experiments and an elastoplastic model with cubic distortional yield surface, Journal of Engineering Mechanics, 148(6), 04022027, 2022.

FISV Since 1982

Simulations of strain-controlled paths $(\epsilon_{zz}, \epsilon_{z\theta}) \rightarrow (0\,\%, 0\%) \rightarrow (0.5\,\%, 0) \rightarrow (0.5\,\%, 0.5\%)$

Strain state (input)

$$\begin{bmatrix} \epsilon_{rr} & \epsilon_{r\theta} & \epsilon_{rz} \\ \epsilon_{r\theta} & \epsilon_{\theta\theta} & \epsilon_{z\theta} \\ \epsilon_{rz} & \epsilon_{z\theta} & \epsilon_{zz} \end{bmatrix} = \begin{bmatrix} 0 & 0 & 0 \\ 0 & 0 & \epsilon_{z\theta} \\ 0 & \epsilon_{z\theta} & \epsilon_{zz} \end{bmatrix}$$

$G = 24.50$ GPa
$E = 69.99$ GPa
$r^l = 0.899$
$r^s = 0.880$
$R^l_\infty = 56.70$ MPa
$R^s_\infty = 39.90$ MPa
$G^l_p = 8.43$ GPa
$G^s_p = 28.72$ GPa
$\eta_l = 48.27$ MPa
$\eta_s = 38.69$ MPa

↓

Model

↓

Stress state (output)

$$\begin{bmatrix} \sigma_{rr} & \sigma_{r\theta} & \sigma_{rz} \\ \sigma_{r\theta} & \sigma_{\theta\theta} & \sigma_{z\theta} \\ \sigma_{rz} & \sigma_{z\theta} & \sigma_{zz} \end{bmatrix} = \begin{bmatrix} \sigma_{rr} & \sigma_{r\theta} & \sigma_{rz} \\ \sigma_{r\theta} & \sigma_{\theta\theta} & \sigma_{z\theta} \\ \sigma_{rz} & \sigma_{z\theta} & \sigma_{zz} \end{bmatrix}$$

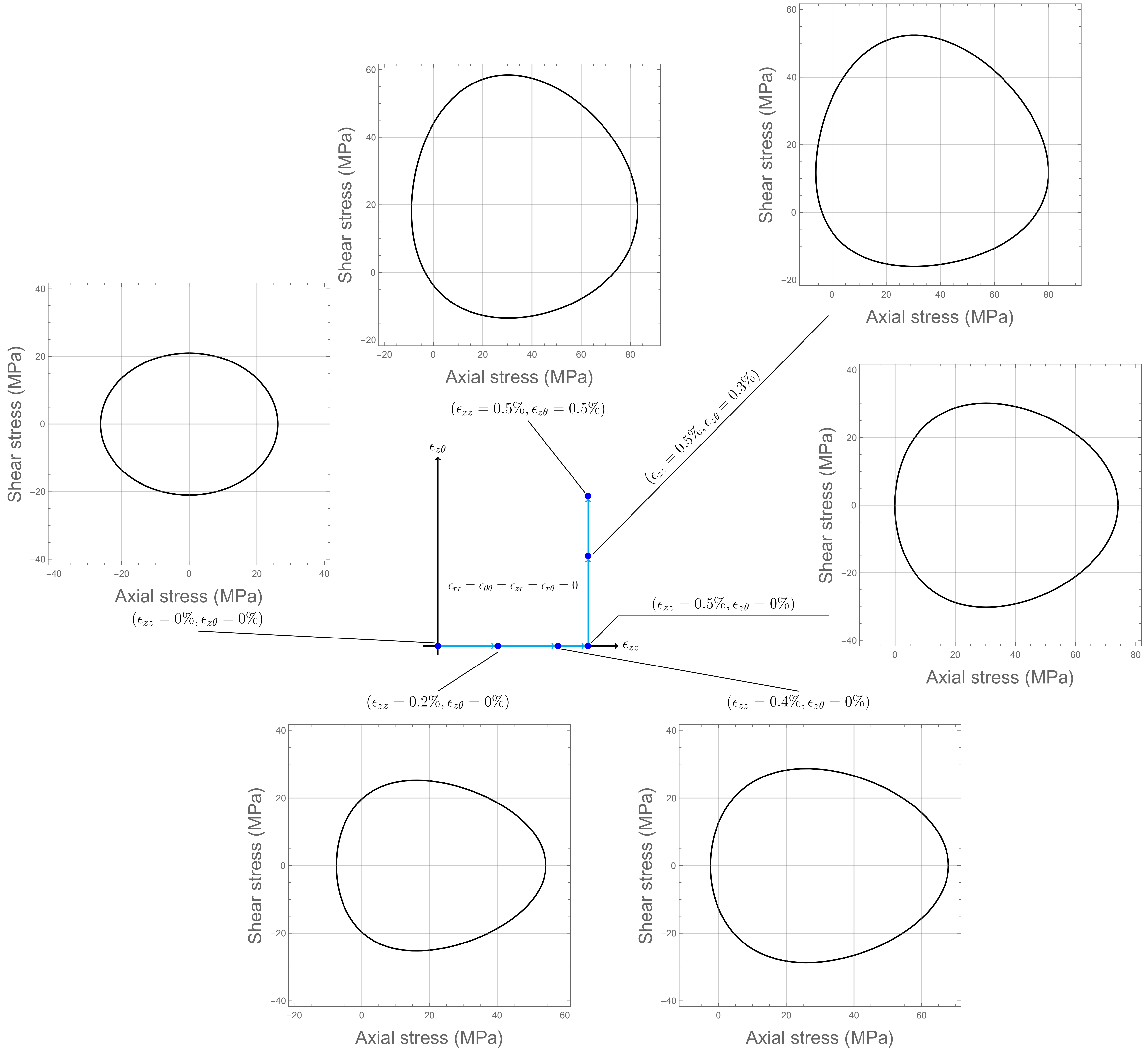

- Hong-Ki Hong, Li-Wei Liu, Ya-Po Shiao, and Shao-Fu Yan, Axial-torsional strain-controlled experiments and an elastoplastic model with cubic distortional yield surface, Journal of Engineering Mechanics, 148(6), 04022027, 2022.

Simulations of strain-controlled paths

$$(\epsilon_{zz}, \epsilon_{z\theta}) \rightarrow (0\,\%\,,0\%) \rightarrow (0\,\%\,,0.5\%) \rightarrow (0.5\,\%\,,0.5\%)$$

Strain state (input)

$$\begin{bmatrix} \epsilon_{rr} & \epsilon_{r\theta} & \epsilon_{rz} \\ \epsilon_{r\theta} & \epsilon_{\theta\theta} & \epsilon_{z\theta} \\ \epsilon_{rz} & \epsilon_{z\theta} & \epsilon_{zz} \end{bmatrix} = \begin{bmatrix} 0 & 0 & 0 \\ 0 & 0 & \epsilon_{z\theta} \\ 0 & \epsilon_{z\theta} & \epsilon_{zz} \end{bmatrix}$$

$$G = 24.50 \text{ GPa}$$
$$E = 69.99 \text{ GPa}$$
$$r^l = 0.899$$
$$r^s = 0.880$$
$$R^l_\infty = 56.70 \text{ MPa}$$
$$R^s_\infty = 39.90 \text{ MPa}$$
$$G^l_p = 8.43 \text{ GPa}$$
$$G^s_p = 28.72 \text{ GPa}$$
$$\eta_l = 48.27 \text{ MPa}$$
$$\eta_s = 38.69 \text{ MPa}$$

Model

Stress state (output)

$$\begin{bmatrix} \sigma_{rr} & \sigma_{r\theta} & \sigma_{rz} \\ \sigma_{r\theta} & \sigma_{\theta\theta} & \sigma_{z\theta} \\ \sigma_{rz} & \sigma_{z\theta} & \sigma_{zz} \end{bmatrix} = \begin{bmatrix} \sigma_{rr} & \sigma_{r\theta} & \sigma_{rz} \\ \sigma_{r\theta} & \sigma_{\theta\theta} & \sigma_{z\theta} \\ \sigma_{rz} & \sigma_{z\theta} & \sigma_{zz} \end{bmatrix}$$

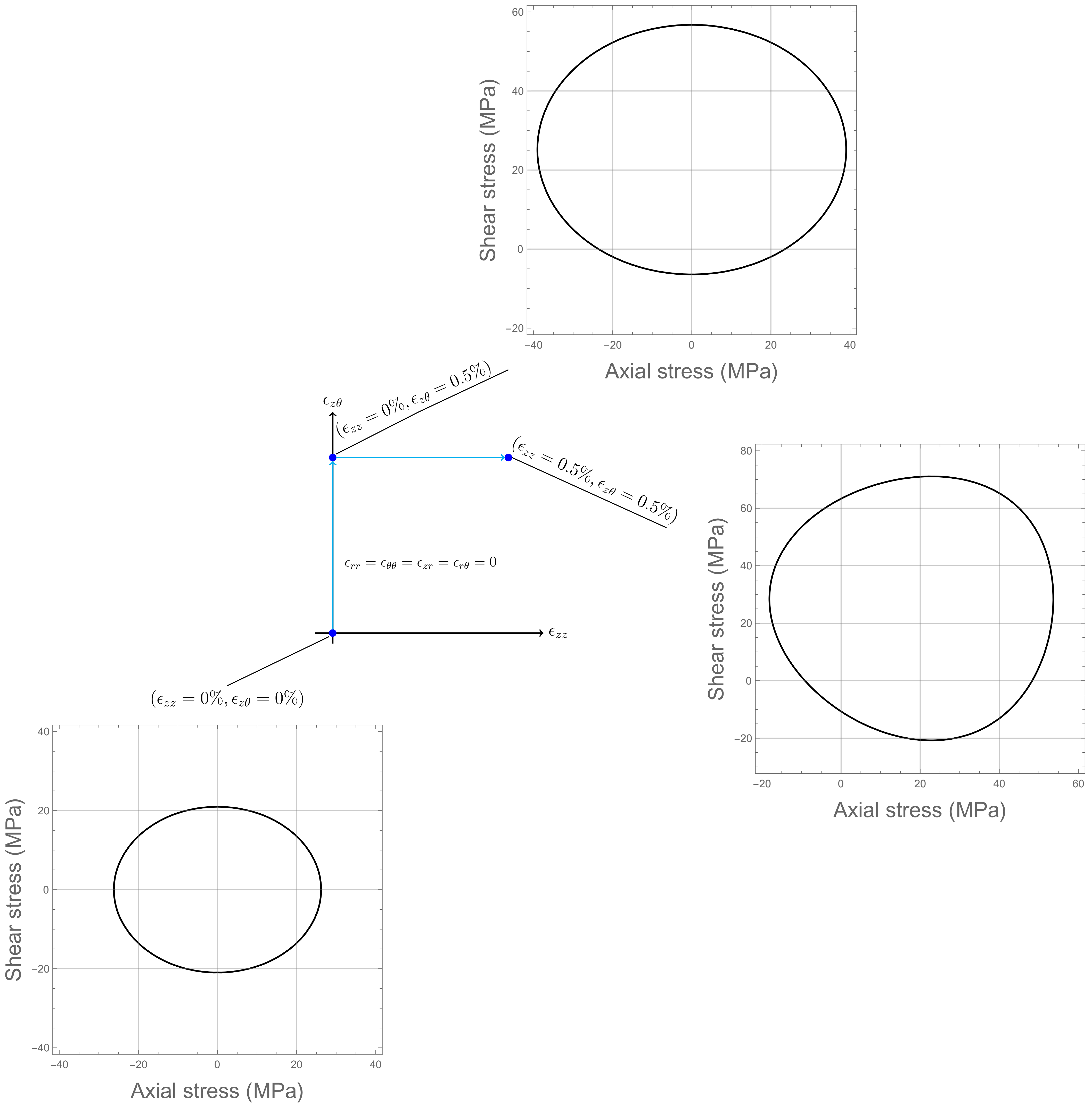

National Taiwan University

- Hong-Ki Hong, Li-Wei Liu, Ya-Po Shiao, and Shao-Fu Yan, Axial-torsional strain-controlled experiments and an elastoplastic model with cubic distortional yield surface, Journal of Engineering Mechanics, 148(6), 04022027, 2022.

FISV Since 1982

Simulations of strain-controlled paths $(\epsilon_{zz}, \epsilon_{z\theta}) \rightarrow (0\,\%, 0\%) \rightarrow (0.4\,\%, 0.4\%)$

Strain state (input)

$$\begin{bmatrix} \epsilon_{rr} & \epsilon_{r\theta} & \epsilon_{rz} \\ \epsilon_{r\theta} & \epsilon_{\theta\theta} & \epsilon_{z\theta} \\ \epsilon_{rz} & \epsilon_{z\theta} & \epsilon_{zz} \end{bmatrix} = \begin{bmatrix} 0 & 0 & 0 \\ 0 & 0 & \epsilon_{z\theta} \\ 0 & \epsilon_{z\theta} & \epsilon_{zz} \end{bmatrix}$$

$G = 24.50$ GPa
$E = 69.99$ GPa
$r^l = 0.899$
$r^s = 0.880$
$R^l_\infty = 56.70$ MPa
$R^s_\infty = 39.90$ MPa
$G^l_p = 8.43$ GPa
$G^s_p = 28.72$ GPa
$\eta_l = 48.27$ MPa
$\eta_s = 38.69$ MPa

Model

Stress state (output)

$$\begin{bmatrix} \sigma_{rr} & \sigma_{r\theta} & \sigma_{rz} \\ \sigma_{r\theta} & \sigma_{\theta\theta} & \sigma_{z\theta} \\ \sigma_{rz} & \sigma_{z\theta} & \sigma_{zz} \end{bmatrix} = \begin{bmatrix} \sigma_{rr} & \sigma_{r\theta} & \sigma_{rz} \\ \sigma_{r\theta} & \sigma_{\theta\theta} & \sigma_{z\theta} \\ \sigma_{rz} & \sigma_{z\theta} & \sigma_{zz} \end{bmatrix}$$

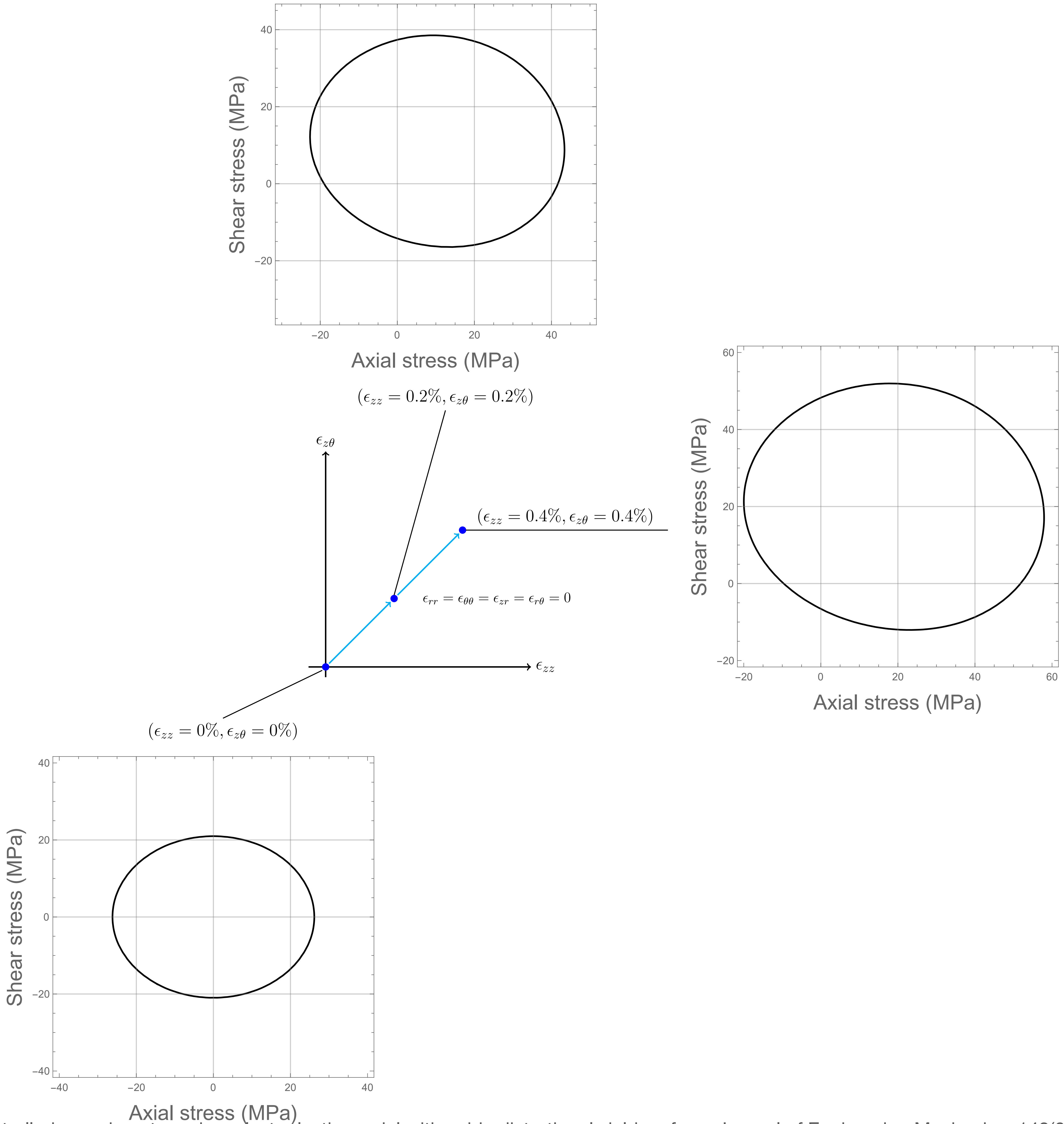

- Hong-Ki Hong, Li-Wei Liu, Ya-Po Shiao, and Shao-Fu Yan, Axial-torsional strain-controlled experiments and an elastoplastic model with cubic distortional yield surface, Journal of Engineering Mechanics, 148(6), 04022027, 2022.

Yield surface evolution under strain-controlled paths

Equipment in MSV lab

MTS system
axial load: max ±500 kN
torque: max ±5500 N-m

axial-torsional extensometer

self-made hydraulic system
internal pressure: max 68.65 MPa

Specimens and control system

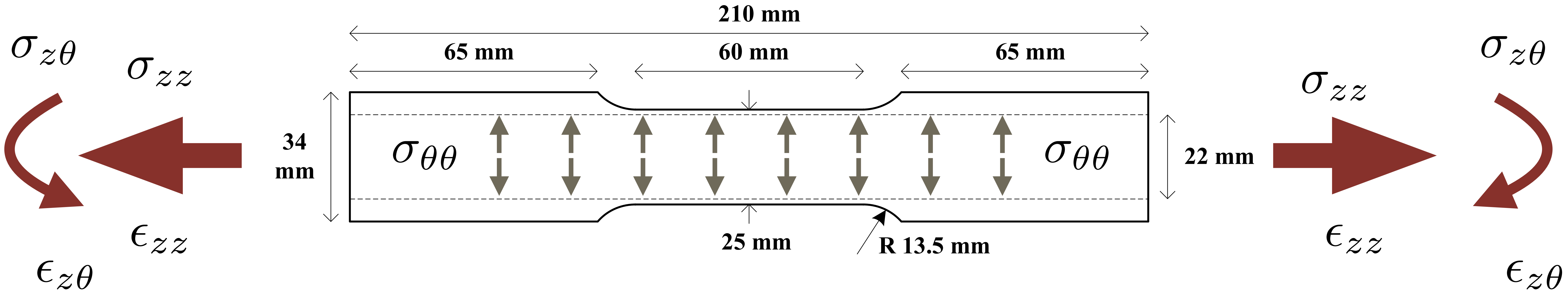

pre-loading space

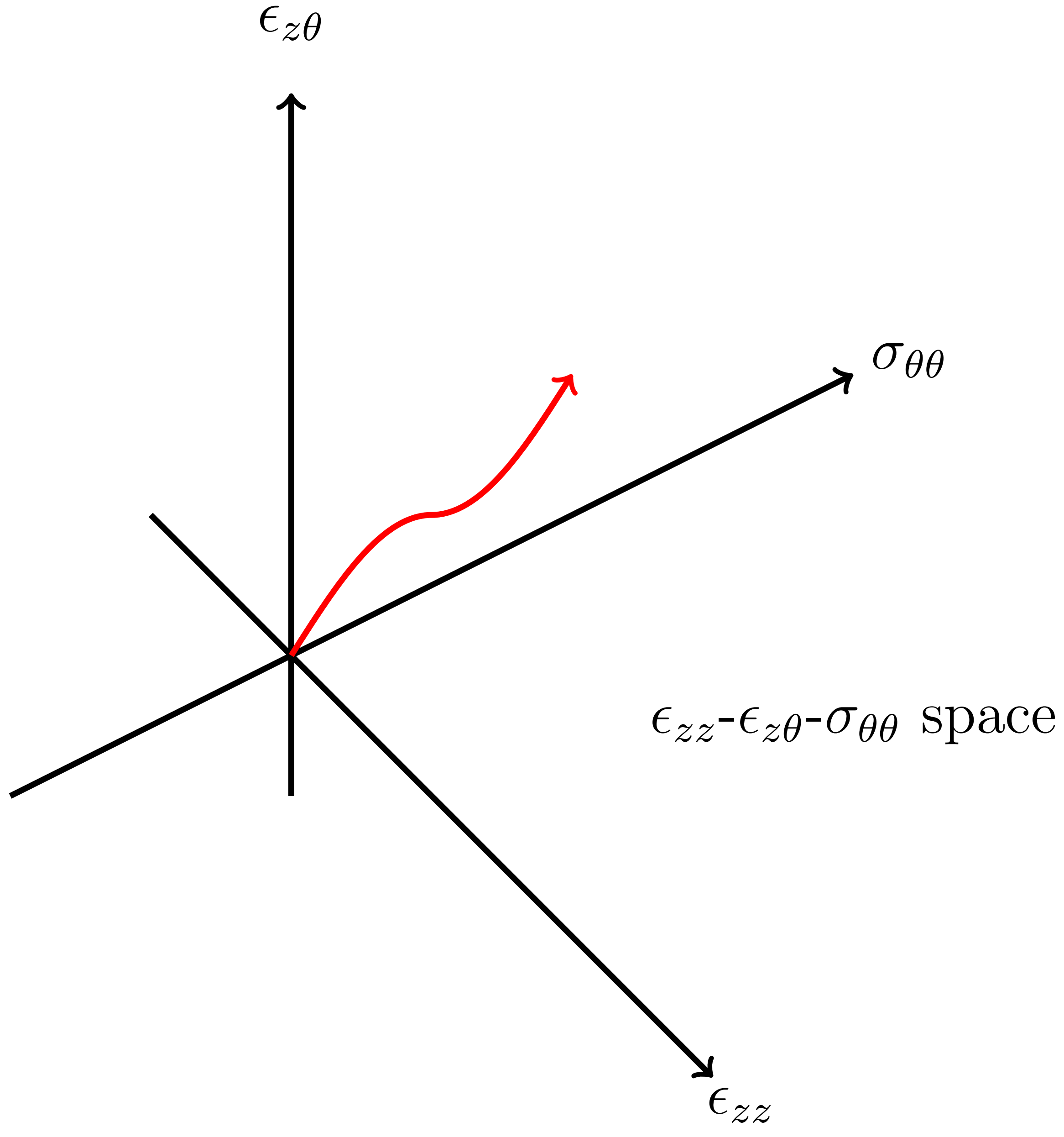

detection planes

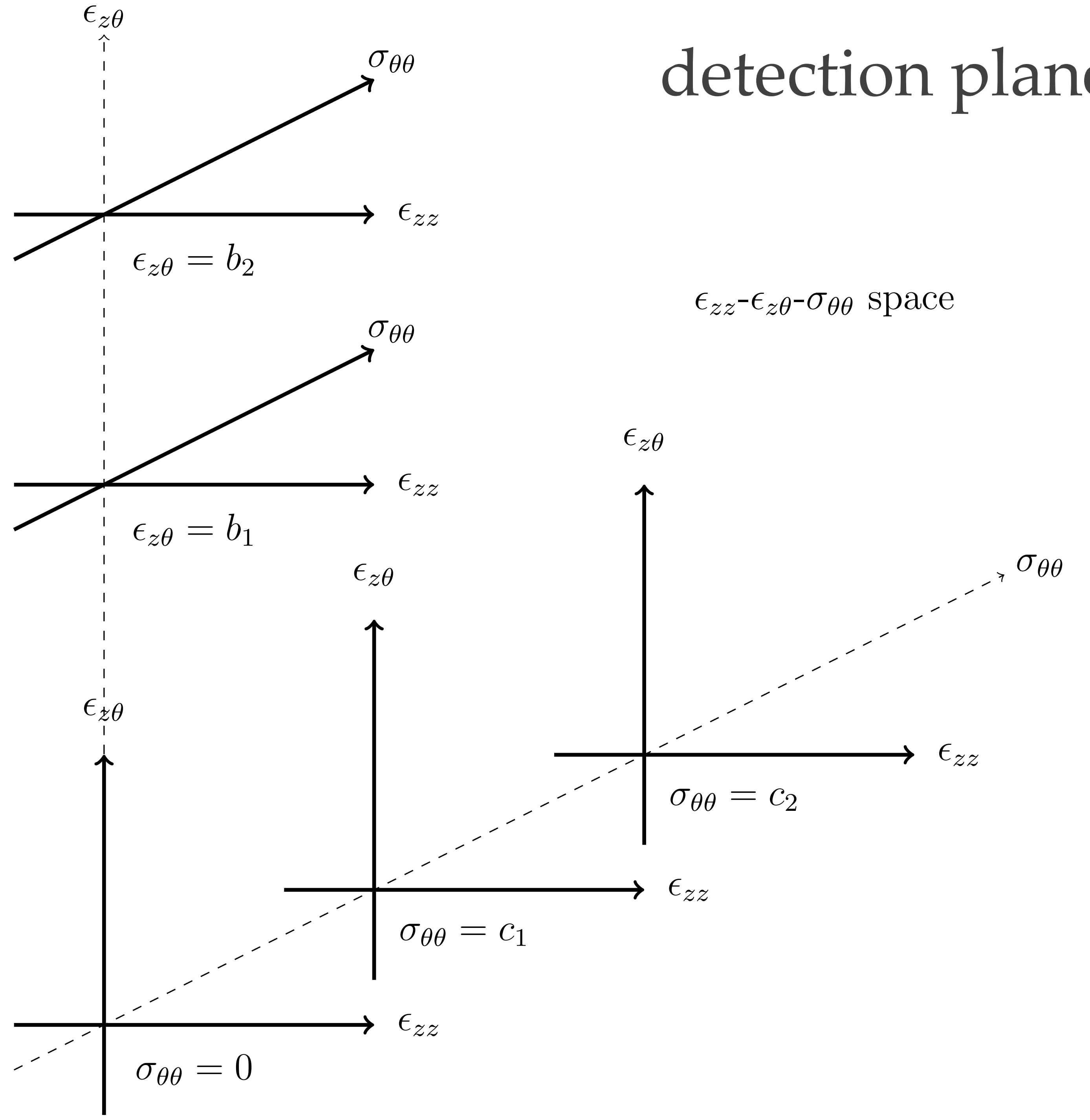

Performance of the yield function in axial-torsional strain-controlled experiments

An axial pre-strain followed by a torsional pre-strain

$$(\epsilon_{zz}, \epsilon_{z\theta}) \rightarrow (0\,\%, 0\%) \rightarrow (0.5\,\%, 0) \rightarrow (0.5\,\%, 0.5\%)$$

Stress state

$$\begin{bmatrix} \sigma_{rr} & \sigma_{r\theta} & \sigma_{rz} \\ \sigma_{r\theta} & \sigma_{\theta\theta} & \sigma_{z\theta} \\ \sigma_{rz} & \sigma_{z\theta} & \sigma_{zz} \end{bmatrix} = \begin{bmatrix} 0 & 0 & 0 \\ 0 & 0 & \sigma_{z\theta} \\ 0 & \sigma_{z\theta} & \sigma_{zz} \end{bmatrix}$$

Strain state

$$\begin{bmatrix} \epsilon_{rr} & \epsilon_{r\theta} & \epsilon_{rz} \\ \epsilon_{r\theta} & \epsilon_{\theta\theta} & \epsilon_{z\theta} \\ \epsilon_{rz} & \epsilon_{z\theta} & \epsilon_{zz} \end{bmatrix} = \begin{bmatrix} \epsilon_{rr} & 0 & 0 \\ 0 & \epsilon_{\theta\theta} & \epsilon_{z\theta} \\ 0 & \epsilon_{z\theta} & \epsilon_{zz} \end{bmatrix}$$

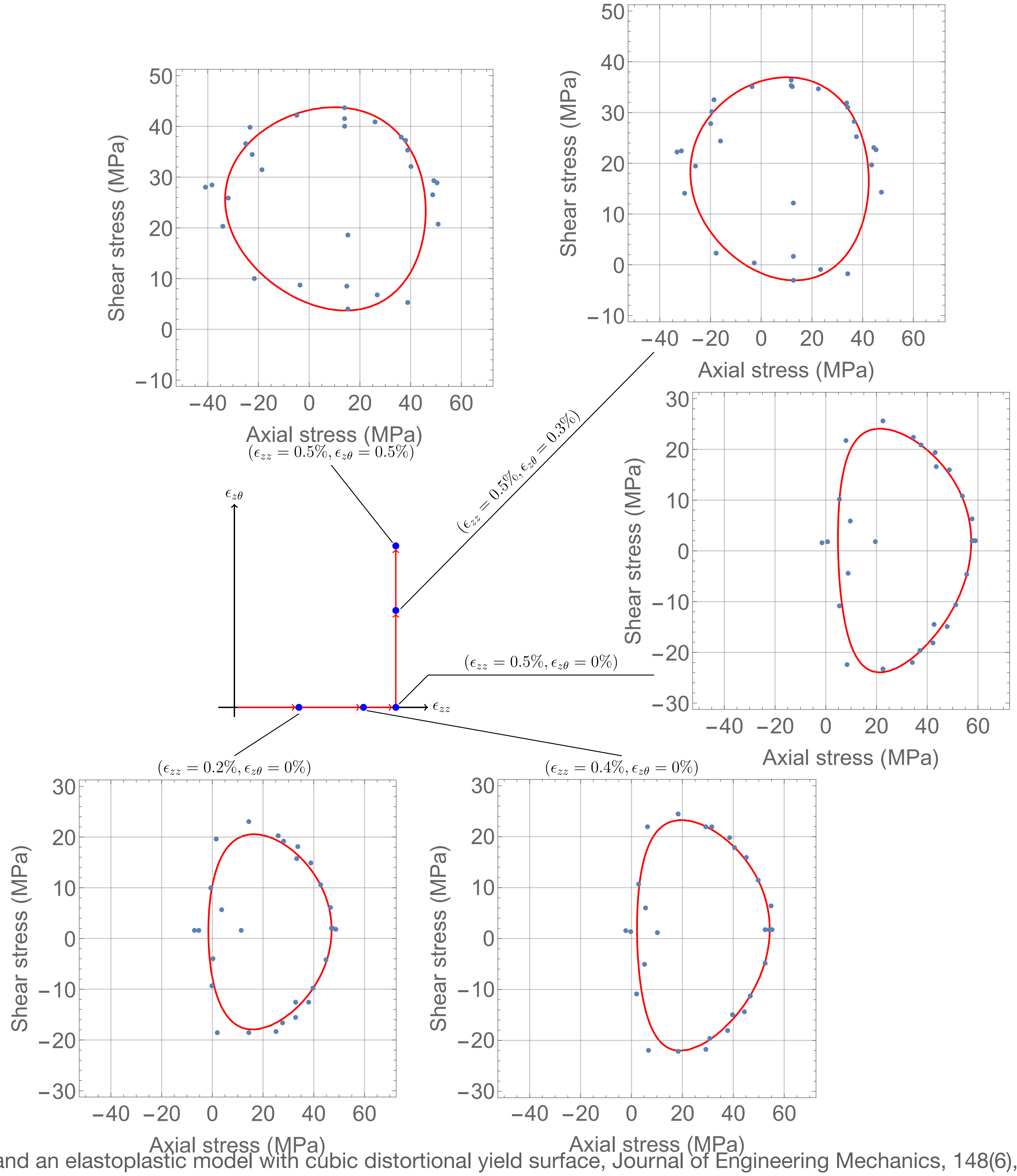

- Hong-Ki Hong, Li-Wei Liu, Ya-Po Shiao, and Shao-Fu Yan, Axial-torsional strain-controlled experiments and an elastoplastic model with cubic distortional yield surface, Journal of Engineering Mechanics, 148(6), 04022027, 2022.

Performance of the yield function in axial-torsional strain-controlled experiments

An torsional pre-strain followed by an axial pre-strain

$(\epsilon_{zz}, \epsilon_{z\theta}) \rightarrow (0\,\%, 0\%) \rightarrow (0\,\%, 0.5\%) \rightarrow (0.5\,\%, 0.5\%)$

Stress state

$$\begin{bmatrix} \sigma_{rr} & \sigma_{r\theta} & \sigma_{rz} \\ \sigma_{r\theta} & \sigma_{\theta\theta} & \sigma_{z\theta} \\ \sigma_{rz} & \sigma_{z\theta} & \sigma_{zz} \end{bmatrix} = \begin{bmatrix} 0 & 0 & 0 \\ 0 & 0 & \sigma_{z\theta} \\ 0 & \sigma_{z\theta} & \sigma_{zz} \end{bmatrix}$$

Strain state

$$\begin{bmatrix} \epsilon_{rr} & \epsilon_{r\theta} & \epsilon_{rz} \\ \epsilon_{r\theta} & \epsilon_{\theta\theta} & \epsilon_{z\theta} \\ \epsilon_{rz} & \epsilon_{z\theta} & \epsilon_{zz} \end{bmatrix} = \begin{bmatrix} \epsilon_{rr} & 0 & 0 \\ 0 & \epsilon_{\theta\theta} & \epsilon_{z\theta} \\ 0 & \epsilon_{z\theta} & \epsilon_{zz} \end{bmatrix}$$

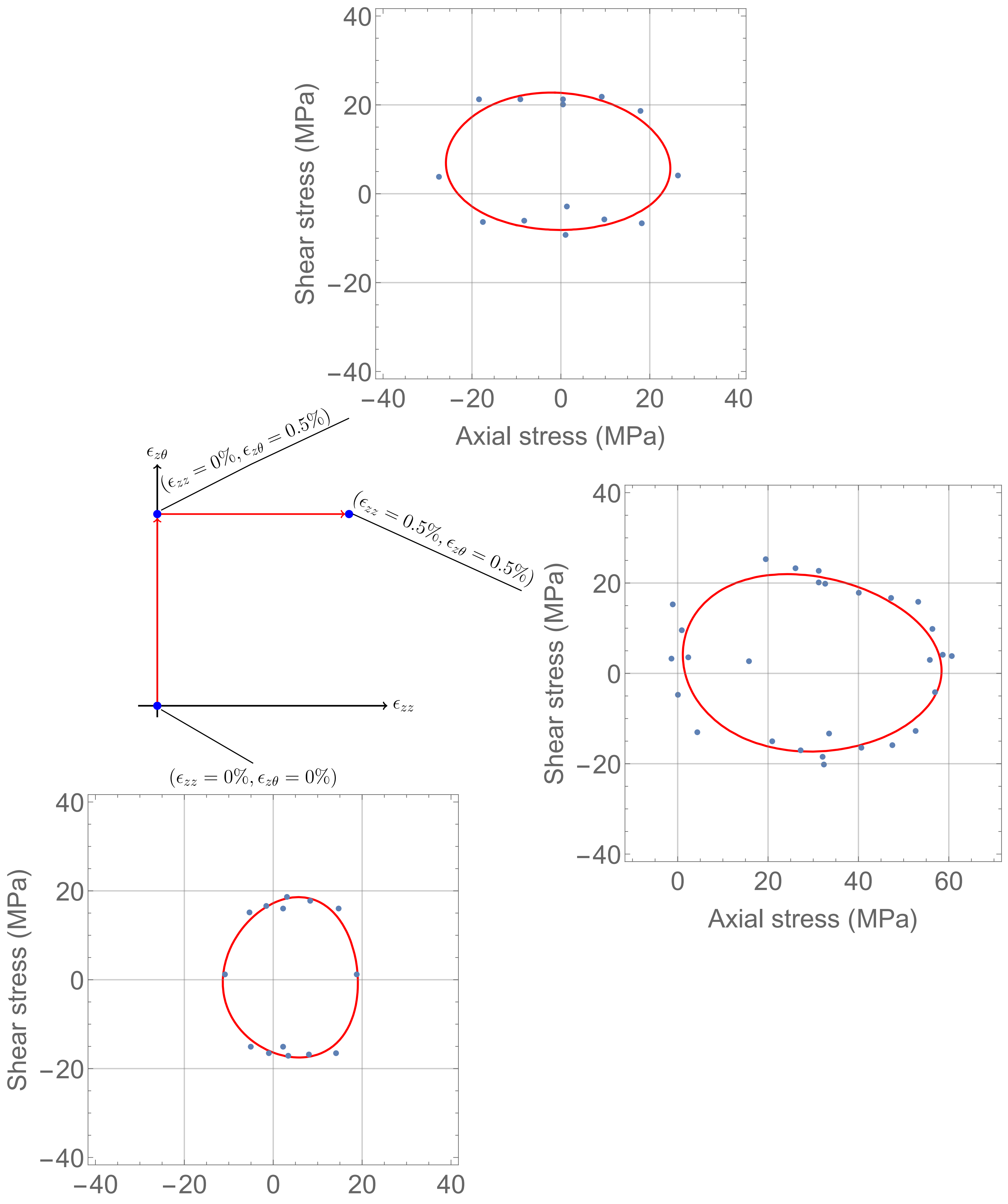

- Hong-Ki Hong, Li-Wei Liu, Ya-Po Shiao, and Shao-Fu Yan, Axial-torsional strain-controlled experiments and an elastoplastic model with cubic distortional yield surface, Journal of Engineering Mechanics, 148(6), 04022027, 2022.

Performance of the yield function in axial-torsional strain-controlled experiments

An axial-torsional pre-strain

$(\epsilon_{zz}, \epsilon_{z\theta}) \rightarrow (0\,\%, 0\%) \rightarrow (0.4\,\%, 0.4\%)$

Stress state

$$\begin{bmatrix} \sigma_{rr} & \sigma_{r\theta} & \sigma_{rz} \\ \sigma_{r\theta} & \sigma_{\theta\theta} & \sigma_{z\theta} \\ \sigma_{rz} & \sigma_{z\theta} & \sigma_{zz} \end{bmatrix} = \begin{bmatrix} 0 & 0 & 0 \\ 0 & 0 & \sigma_{z\theta} \\ 0 & \sigma_{z\theta} & \sigma_{zz} \end{bmatrix}$$

Strain state

$$\begin{bmatrix} \epsilon_{rr} & \epsilon_{r\theta} & \epsilon_{rz} \\ \epsilon_{r\theta} & \epsilon_{\theta\theta} & \epsilon_{z\theta} \\ \epsilon_{rz} & \epsilon_{z\theta} & \epsilon_{zz} \end{bmatrix} = \begin{bmatrix} \epsilon_{rr} & 0 & 0 \\ 0 & \epsilon_{\theta\theta} & \epsilon_{z\theta} \\ 0 & \epsilon_{z\theta} & \epsilon_{zz} \end{bmatrix}$$

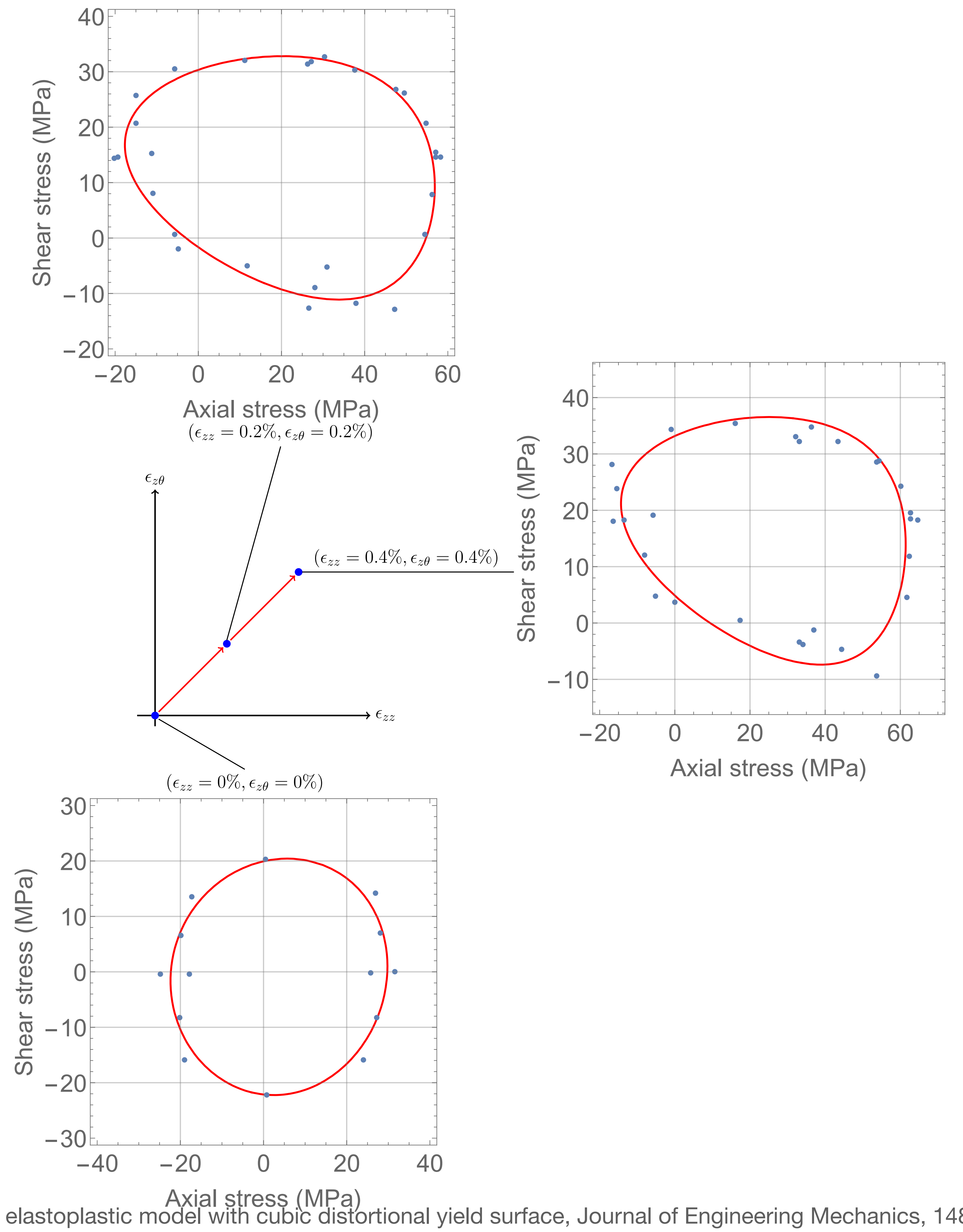

- Hong-Ki Hong, Li-Wei Liu, Ya-Po Shiao, and Shao-Fu Yan, Axial-torsional strain-controlled experiments and an elastoplastic model with cubic distortional yield surface, Journal of Engineering Mechanics, 148(6), 04022027, 2022.

國立臺灣大學 National Taiwan University

HSV Since 1982

Yield surface evolution under stress-controlled paths

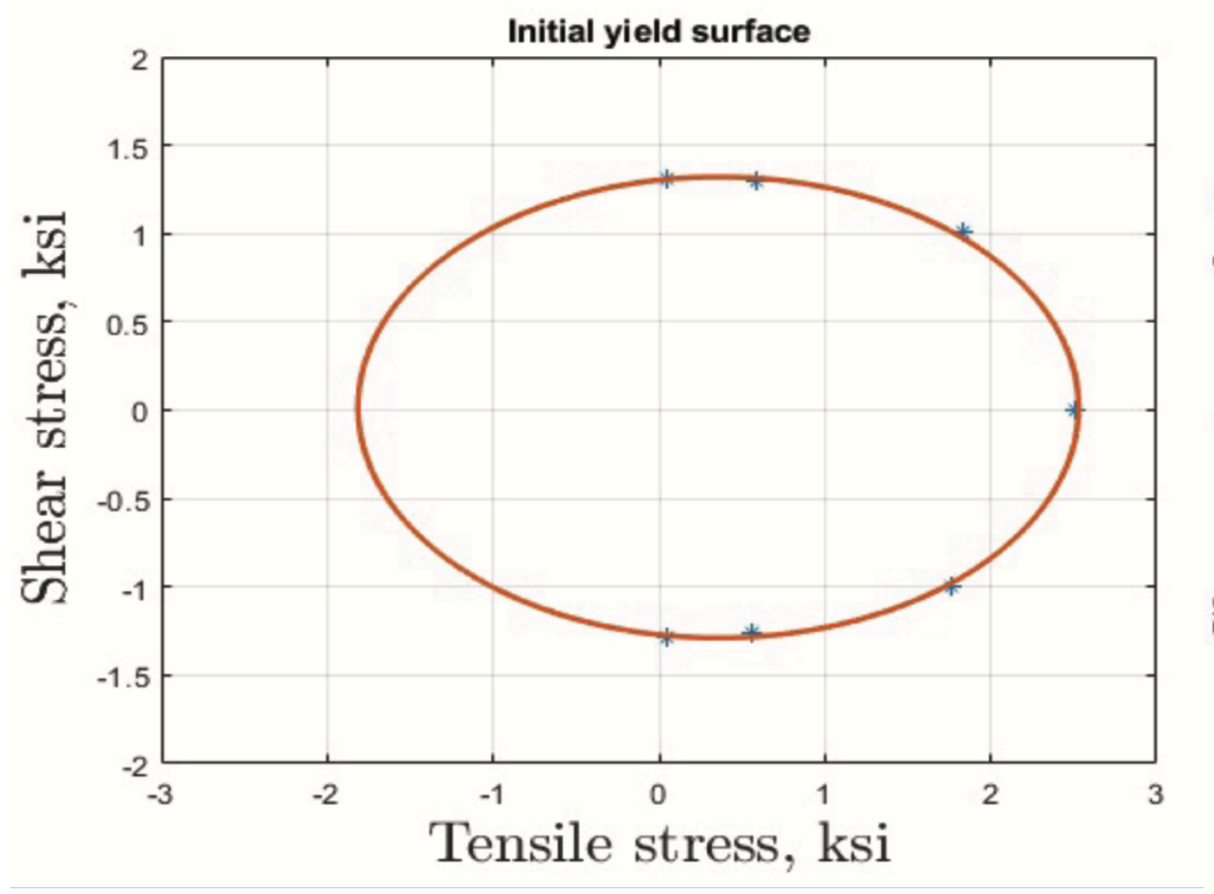

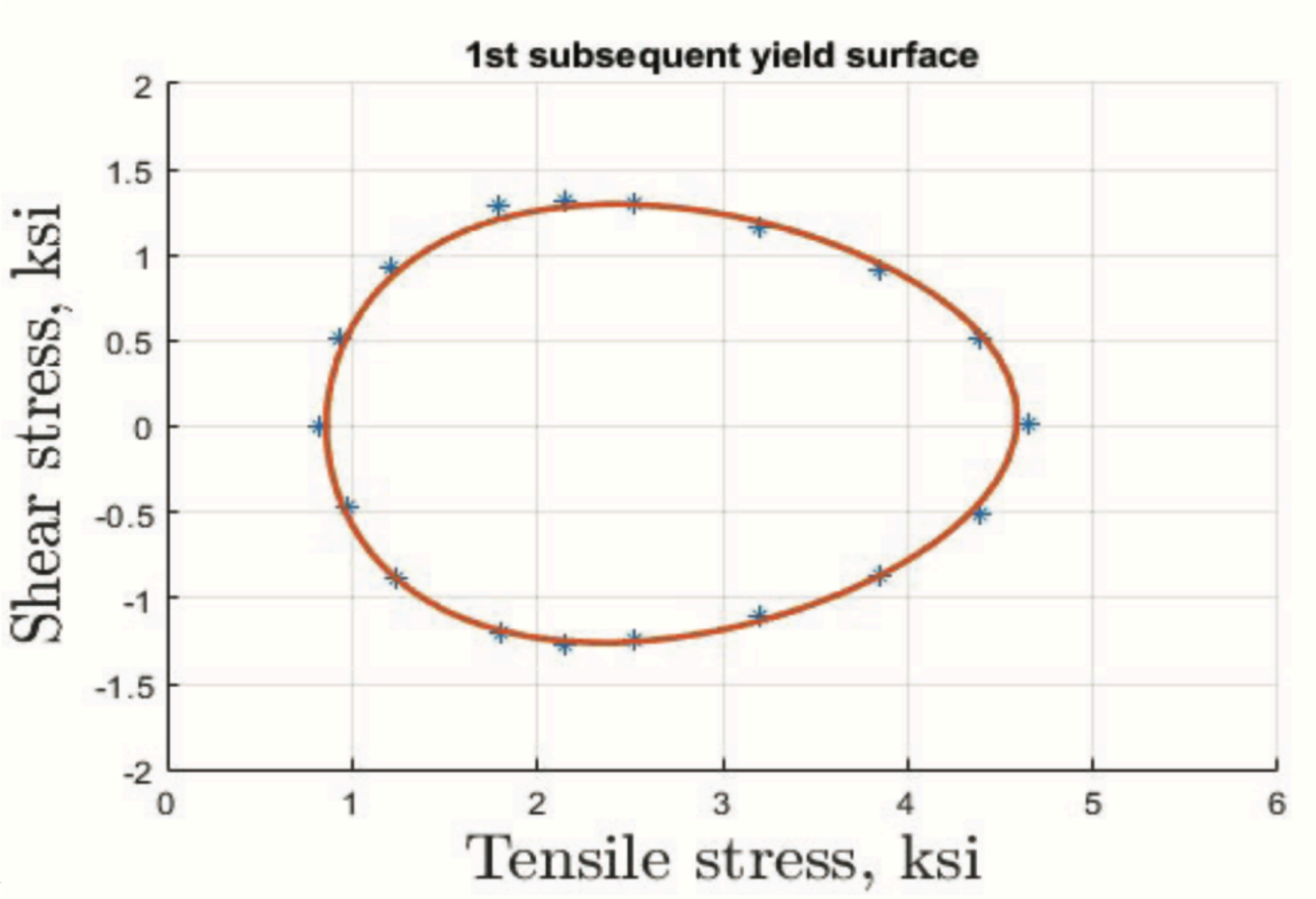

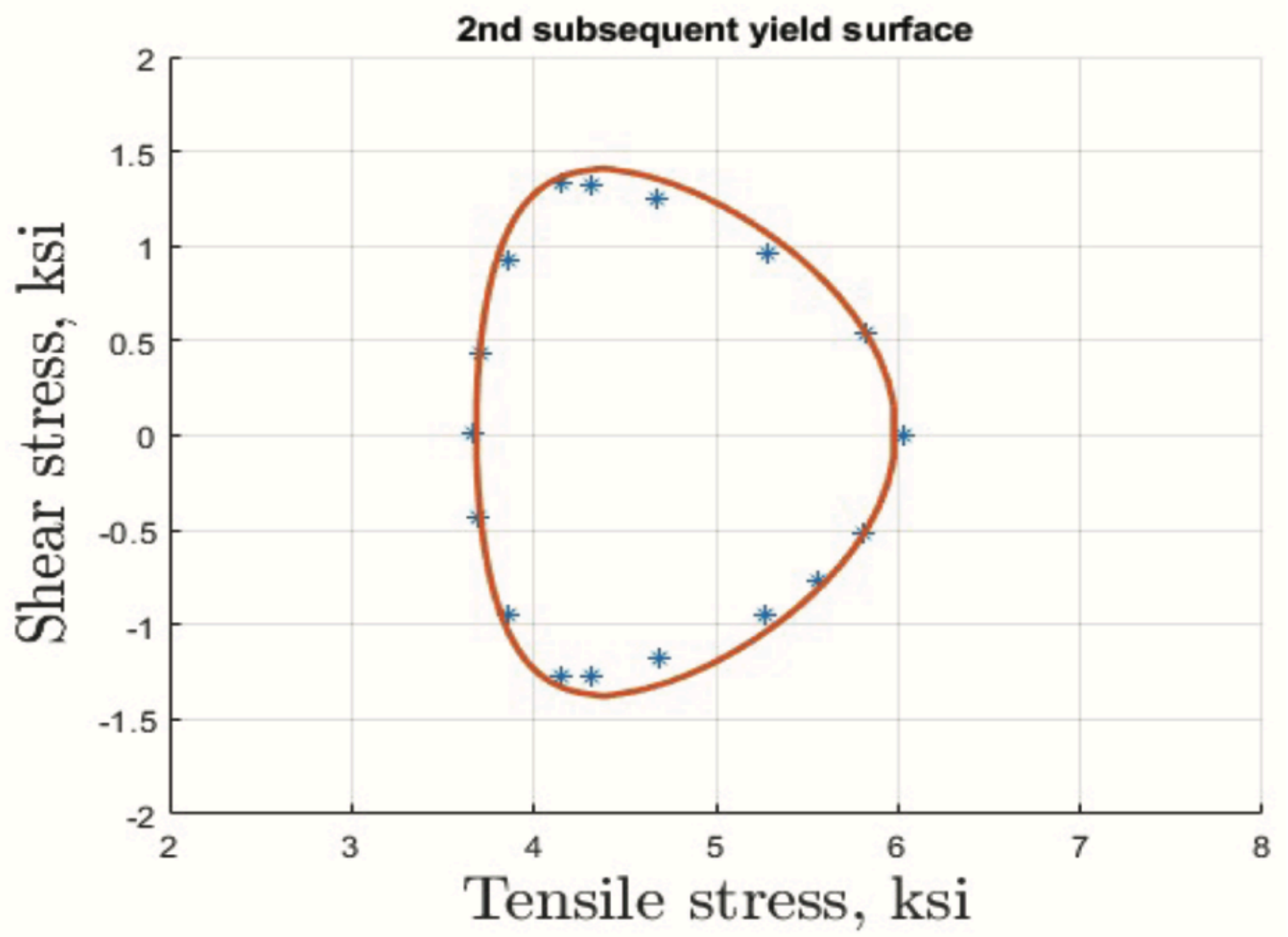

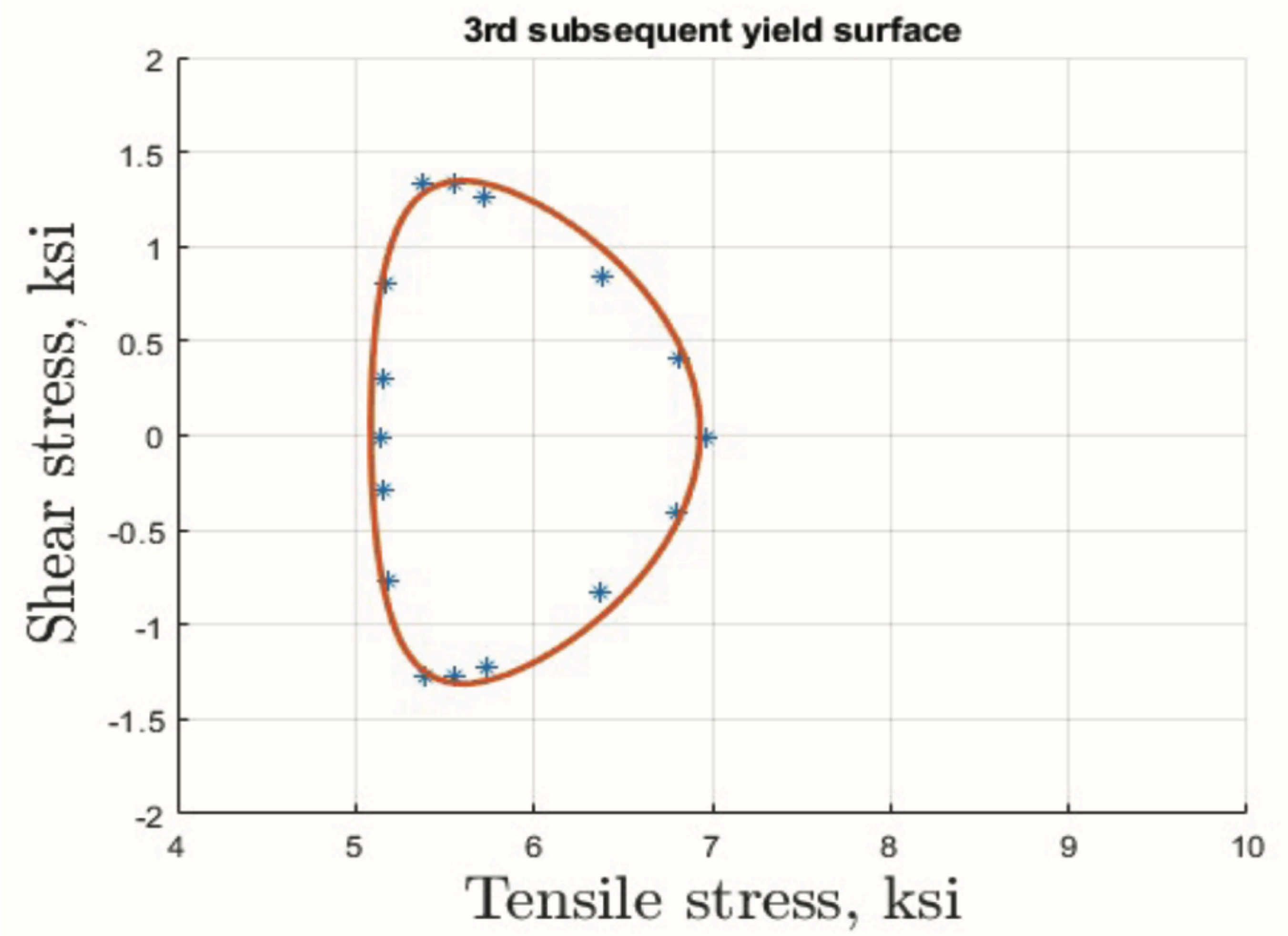

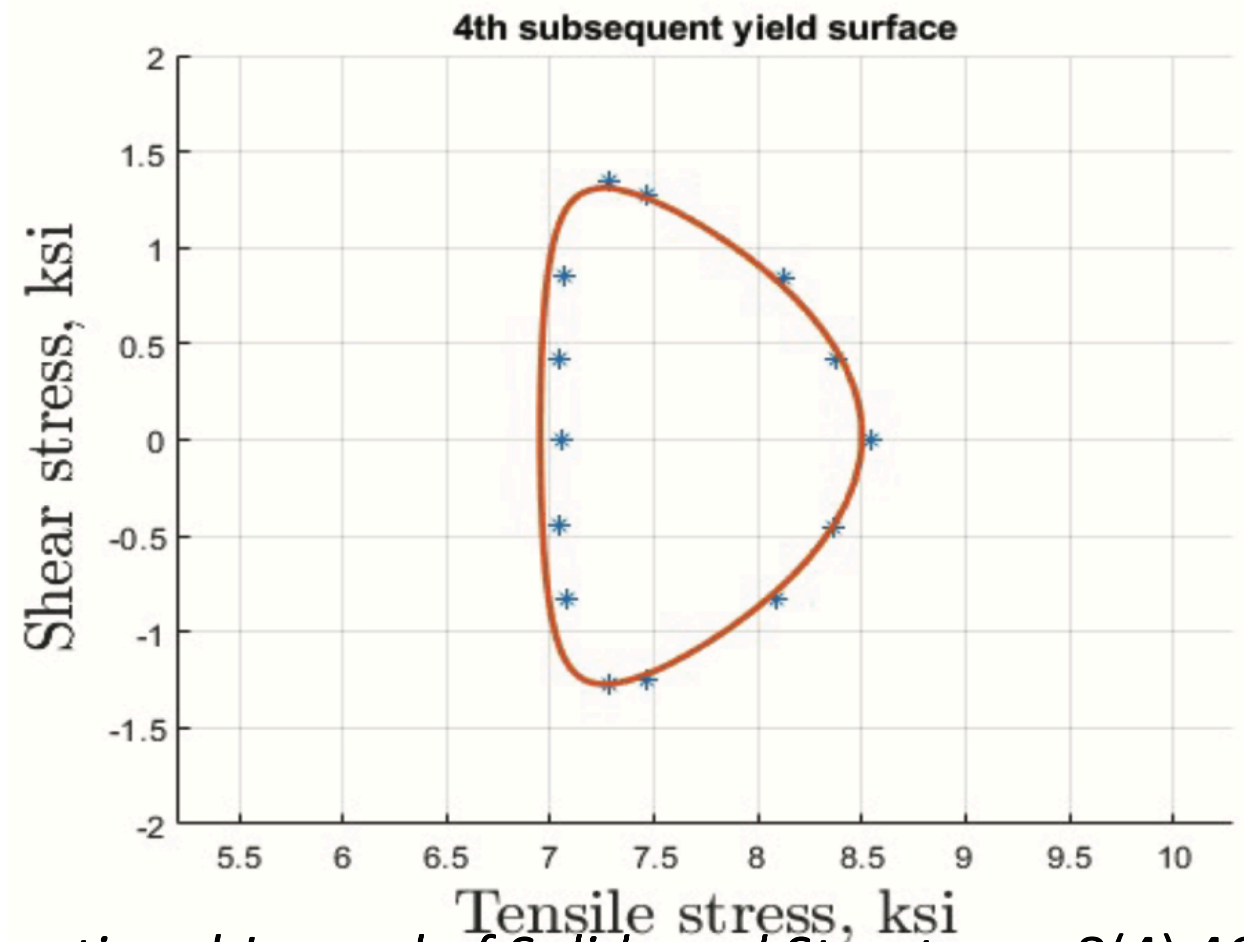

A. Phillips & J.-L. Tang, The effect of loading path on the yield surface at elevated temperatures. *International Journal of Solids and Structures*, 8(4) 463-474, 1972.
K.-M. Hou, The evolution of cubic distortional yield hypersurfaces in materials of flow elastoplasticity under prestress and at elevated temperatures. MS Thesis, Civil Engrg. Dept., National Taiwan University, 2023.

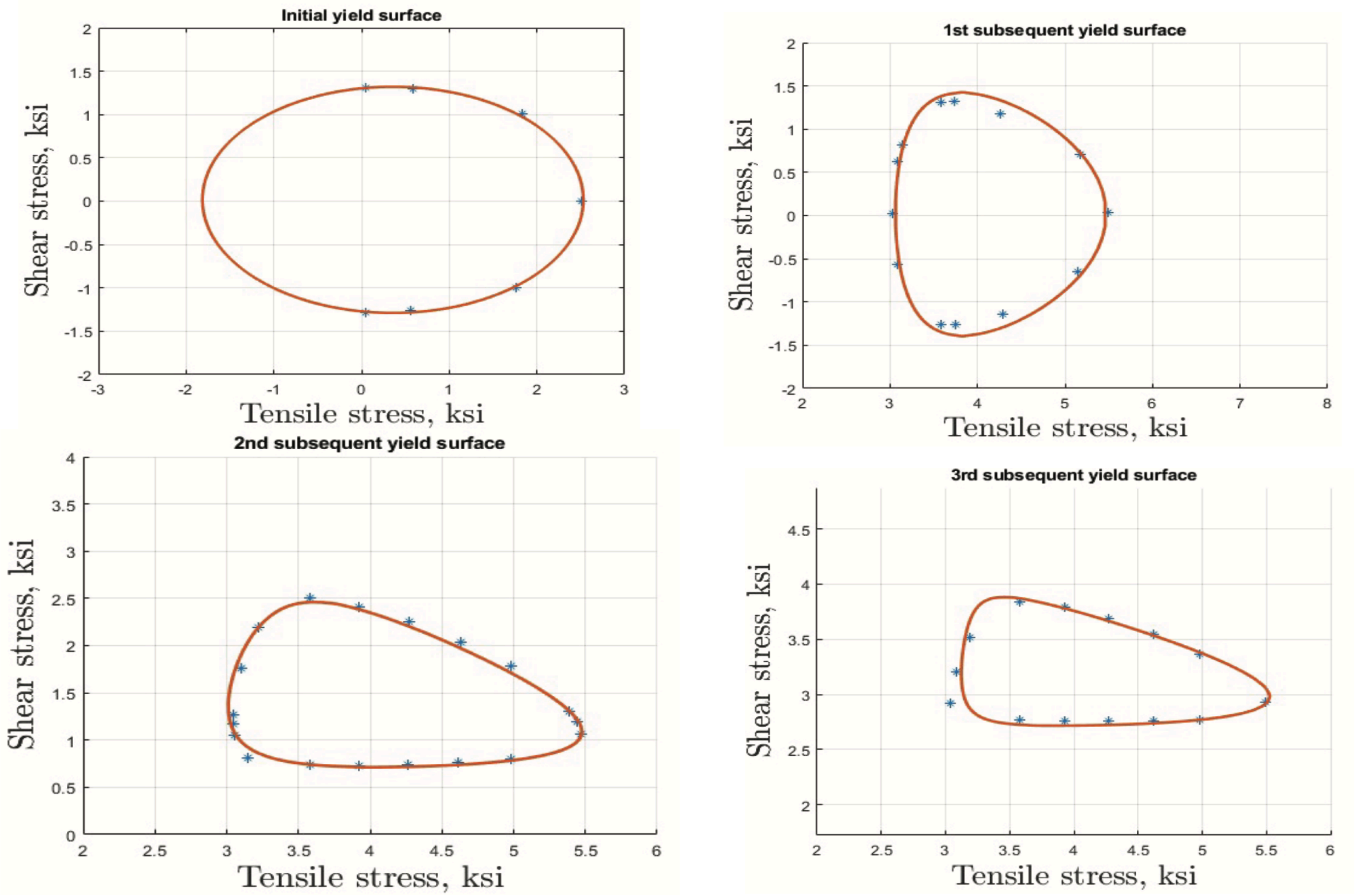

A. Phillips & J.-L. Tang, The effect of loading path on the yield surface at elevated temperatures. *International Journal of Solids and Structures*, 8(4) 463-474, 1972.
K.-M. Hou, The evolution of cubic distortional yield hypersurfaces in materials of flow elastoplasticity under prestress and at elevated temperatures. MS Thesis, Civil Engrg. Dept., National Taiwan University, 2023.

Study of crack of flow elastoplasticity

J-integral

$$J = \int_{-\pi}^{\pi} W n_1 r d\theta - \int_{-\pi}^{\pi} t_i \frac{\partial u_i}{\partial x_1} r d\theta,$$

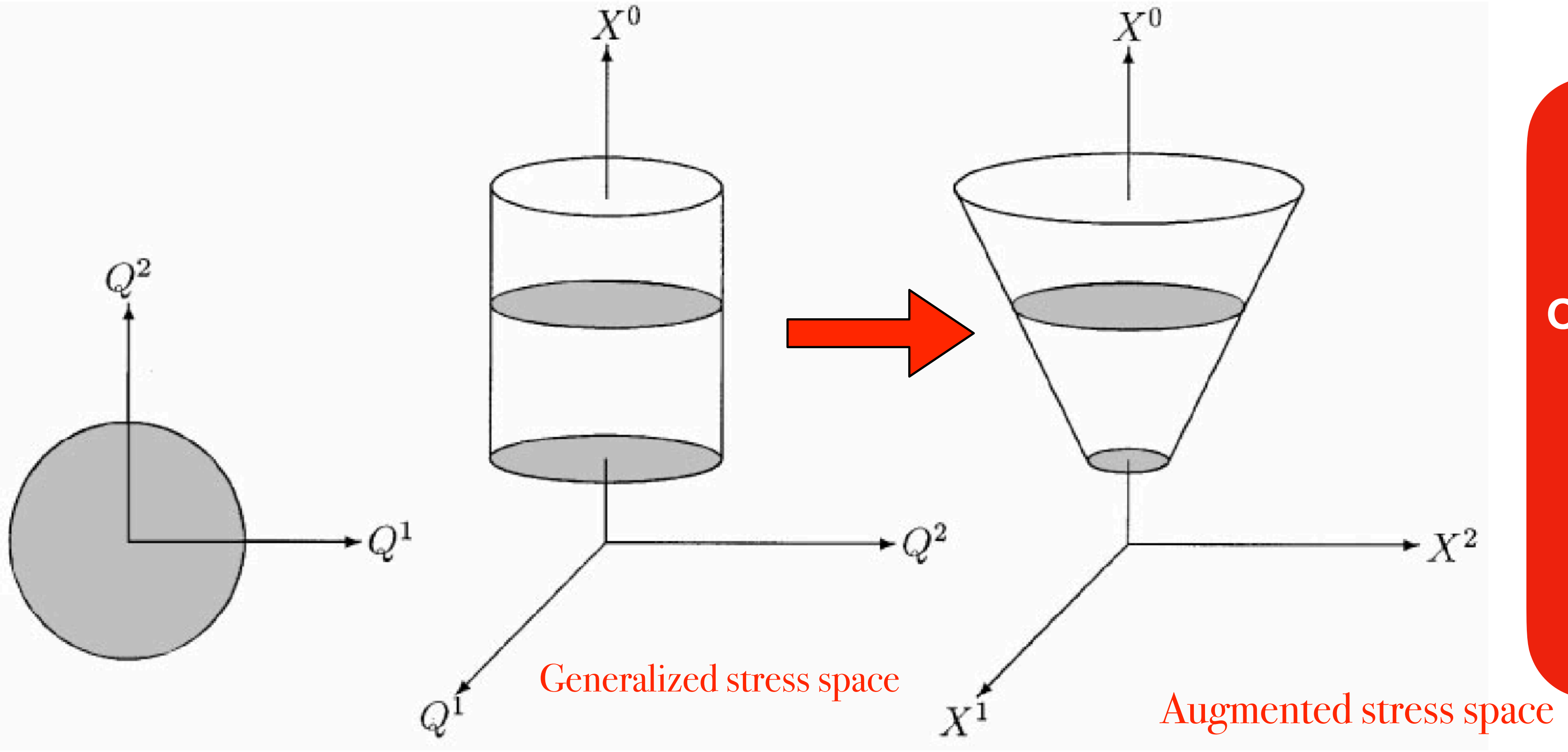

Internal symmetry

Two elements of the proper orthochronous Poincaré group $SE_o(6,1)$ in the plastic phase and one element of the translation group T in the elastic phase

H.-K. Hong and C.-S. Liu.(2000)

$$J(t,r) = \int_{-\pi}^{\pi}\int_0^t \sigma_{ij}(\tau,r,\theta)\dot{\epsilon}_{ij}(\tau,r,\theta) n_1 r d\tau d\theta - \int_{-\pi}^{\pi} t_i(t,r,\theta)\frac{\partial u_i}{\partial x_1}(t,r,\theta) r d\theta$$

$$= \sum_{j=1}^{M}\sum_{k=1}^{N}\int_{t_j}^{t_{j+1}}\int_{\theta_k}^{\theta_k+\Delta\theta\tau} \sigma_{ij}(\tau,r,\theta)\dot{\epsilon}_{ij}(\tau,r,\theta) n_1 r d\theta d\tau$$

$$-\int_{-\pi}^{\pi} t_i(t,r,\theta)\frac{\partial u_i}{\partial x_1}(t,r,\theta) r d\theta$$

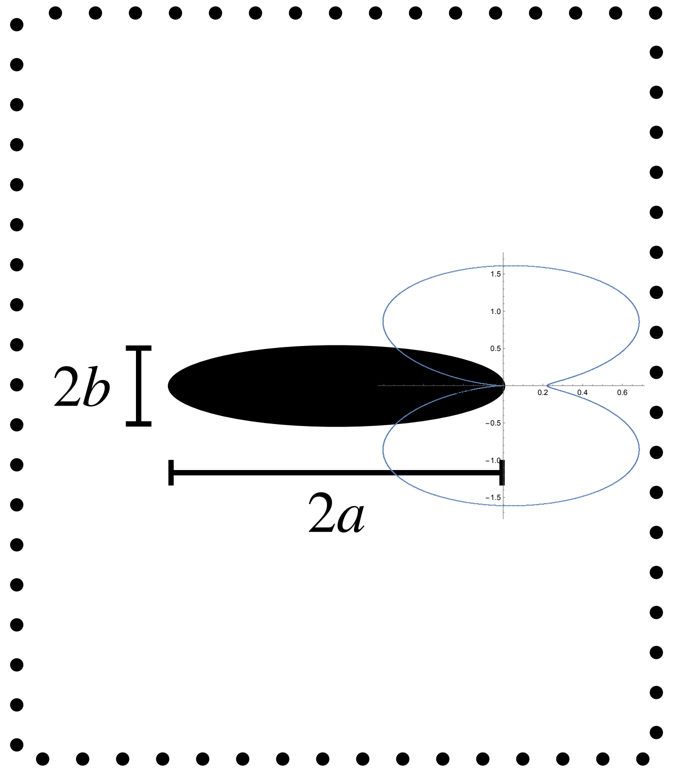

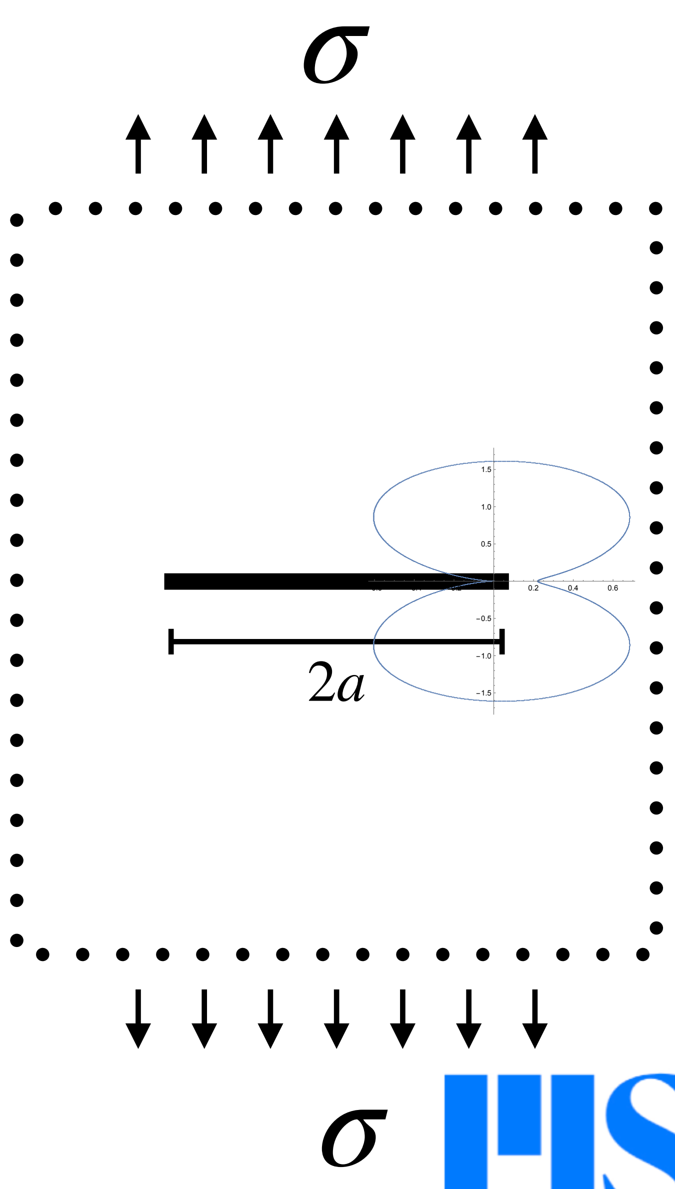

J-integral of flow elastoplasticity

Equivalent plastic strain λ at differ time instant

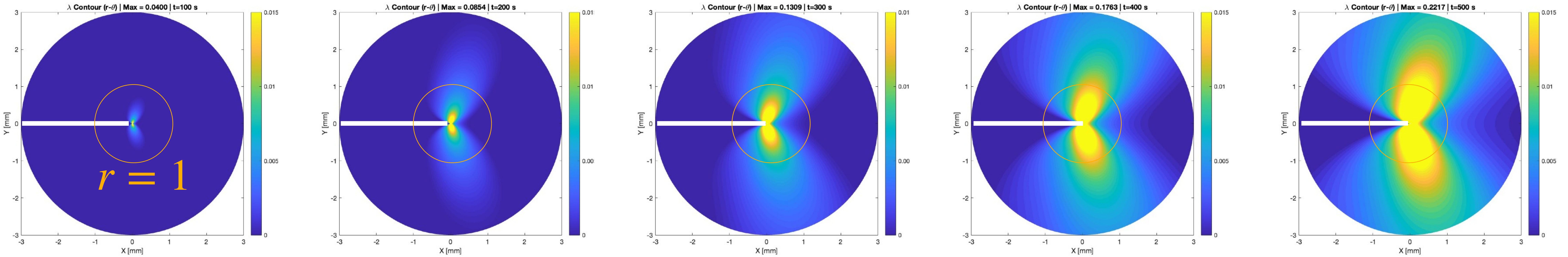

λ at t= 100 s | λ at t=200 s | λ at t=300 s | λ at t=400 s | λ at t=500 s

$J(t,1)$

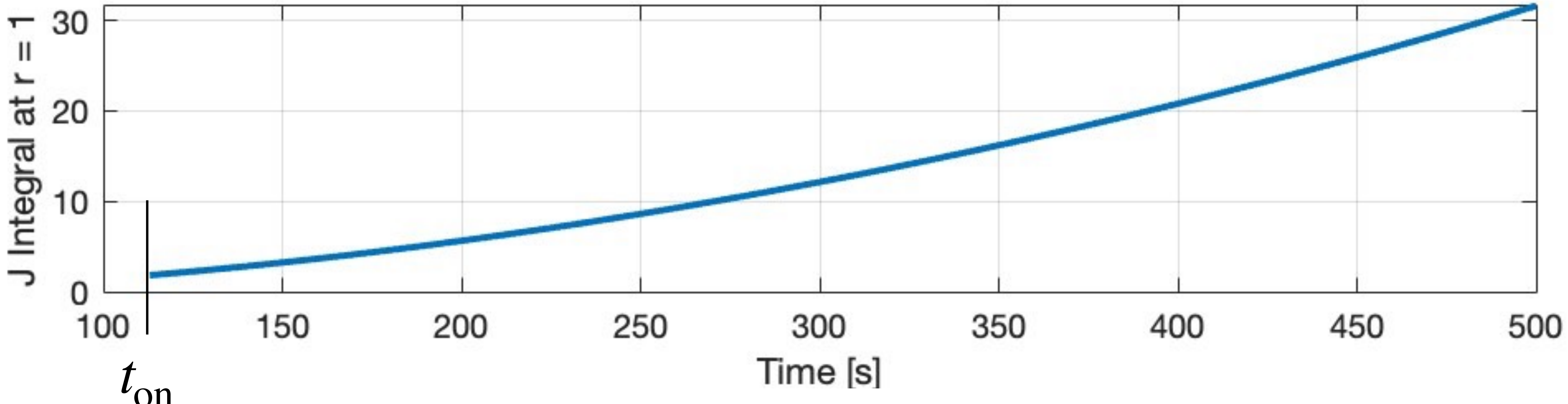

Conclusions

Conclusions

1. By selecting prominent test evidences based upon experiences on aluminium alloy Al6061 gained in our lab [ASCE Journal of Engineering Mechanics 148(6):04022027, 2022] over the course of the years, we created a three-dimensional tensor model of flow elastoplasticity, grasping the axial-torsional experimental features reported in the literature; in particular, in Phillips *et al*. at room and at elevated temperatures on commercially pure aluminium 1100-0.

2. The model needs a total of 8 material constants in addition to Young's modulus and shear modulus and presents an evolving cubic distortion yield hypersurface, which is articulated with two Mises hyperspheres, characteristic of internal symmetry of two elements of the projective proper orthochronous Poincare group in the plastic phase. Associated with each Mises hypersphere in stress space is a normality plastic flow rule of mixed-exp-AF, referring to a combined isotropic-kinematic rule of hardening-softening, which combines the isotropic exponential rule of degree 2 and the kinematic rule of Armstrong-Frederick.

Conclusions

3. By using the model and employing Lie group theory, closed-form exact solutions for rectilinear paths are derived and used to identify a unique set of parameters for fitting successfully evolving shapes of yield surfaces with clear physical meaning.

4. We have applied the solutions to differential segments of the contour path around the crack tip and integrate. Each differential segment is deemed as a straight one, differential though. Upon interchanging the order of the double integration the integration is expected to result in closed-form exact solutions for elastic zone and even for elastoplastic zone.

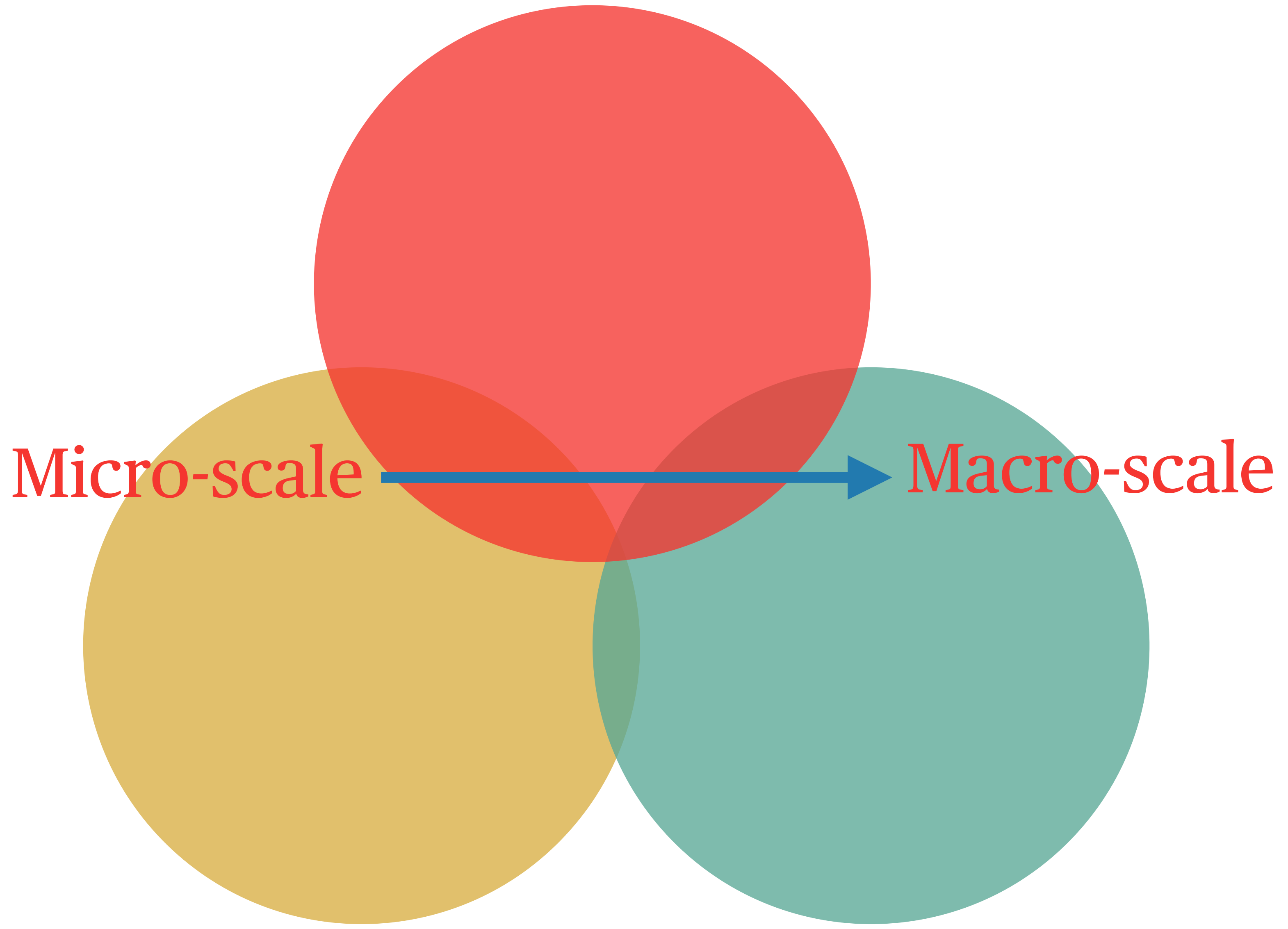

Thanks for your attention

MSV Since 1982

Mechanics, Sound, & Vibration Laboratory

https://davidliulw.wixsite.com/msvlab